

10/20/95

# SANDIA REPORT

SAND95-2060 • UC-600  
Unlimited Release  
Printed September 1995

## SEAMIST™ In-Situ Instrumentation and Vapor Sampling System Applications in the Sandia Mixed Waste Landfill Integrated Demonstration Program: Final Report

Cecelia Williams, William Lowry, David Cremer, Sandra Dalvit Dunn

Prepared by  
Sandia National Laboratories  
Albuquerque, New Mexico 87185 and Livermore, California 94550  
for the United States Department of Energy  
under Contract DE-AC04-94AL85000

Approved for public release; distribution is unlimited.

MASTER

SF2900Q(8-81)

DISTRIBUTION OF THIS DOCUMENT IS UNLIMITED

01

Issued by Sandia National Laboratories, operated for the United States Department of Energy by Sandia Corporation.

**NOTICE:** This report was prepared as an account of work sponsored by an agency of the United States Government. Neither the United States Government nor any agency thereof, nor any of their employees, nor any of their contractors, subcontractors, or their employees, makes any warranty, express or implied, or assumes any legal liability or responsibility for the accuracy, completeness, or usefulness of any information, apparatus, product, or process disclosed, or represents that its use would not infringe privately owned rights. Reference herein to any specific commercial product, process, or service by trade name, trademark, manufacturer, or otherwise, does not necessarily constitute or imply its endorsement, recommendation, or favoring by the United States Government, any agency thereof or any of their contractors or subcontractors. The views and opinions expressed herein do not necessarily state or reflect those of the United States Government, any agency thereof or any of their contractors.

Printed in the United States of America. This report has been reproduced directly from the best available copy.

Available to DOE and DOE contractors from  
Office of Scientific and Technical Information  
PO Box 62  
Oak Ridge, TN 37831

Prices available from (615) 576-8401, FTS 626-8401

Available to the public from  
National Technical Information Service  
US Department of Commerce  
5285 Port Royal Rd  
Springfield, VA 22161

NTIS price codes  
Printed copy: A04  
Microfiche copy: A01

## **DISCLAIMER**

**Portions of this document may be illegible in electronic image products. Images are produced from the best available original document.**

**SEAMIST™ In-Situ Instrumentation and Vapor Sampling System  
Applications in the Sandia Mixed Waste Landfill Integrated  
Demonstration Program: Final Report**

**TTP# AL221115**

Cecelia Williams  
Environmental Restoration Technologies  
Sandia National Laboratories  
Albuquerque, NM 87185-5800

William Lowry, David Cremer, and Sandra Dalvit Dunn  
Science & Engineering Associates, Inc.  
Santa Fe, NM 87505

**ABSTRACT**

The SEAMIST™ inverting membrane deployment system has been used successfully at the Mixed Waste Landfill Integrated Demonstration (MWLID) for multipoint vapor sampling, pressure measurement, permeability measurement, sensor integration demonstrations, and borehole lining. Several instruments were deployed inside the SEAMIST™-lined boreholes to detect metals, radionuclides, moisture, and geologic variations. The liner protected the instruments from contamination, maintained support of the uncased borehole wall, and sealed the total borehole from air circulation.

Recent activities included the installation of three multipoint vapor sampling systems and sensor integration systems in 100-foot-deep vertical boreholes. A long term pressure monitoring program has recorded barometric pressure effects at depth with relatively high spatial resolution. The SEAMIST™ system has been integrated with a variety of hydrologic and chemical sensors for in-situ measurements, demonstrating its versatility as an instrument deployment system that allows easy emplacement and removal. Standard SEAMIST™ vapor sampling systems were also integrated with state-of-the-art volatile organic compound analysis technologies. The results and status of these demonstration tests are presented.

**Intentionally Left Blank**

## **ACKNOWLEDGEMENTS**

The authors wish to acknowledge the contributions of time, efforts, and technical expertise by Philip J. Hargis, Jr. and George Laguna.

We also wish to acknowledge the DOE Office of Technology Development and the Mixed Waste Landfill Integrated Demonstration for their sponsorship of this project.

**Intentionally Left Blank**

## CONTENTS

|                                                                    |    |
|--------------------------------------------------------------------|----|
| ACKNOWLEDGEMENTS .....                                             | v  |
| ACRONYMS .....                                                     | ix |
| INTRODUCTION .....                                                 | 1  |
| INTEGRATING SENSORS WITH SEAMIST™ .....                            | 3  |
| GENERAL DESCRIPTION OF THE EXPERIMENT SETTING .....                | 5  |
| PHYSICAL PROCESS SENSOR FIELD DEMONSTRATIONS .....                 | 9  |
| Pressure Sensors .....                                             | 11 |
| Temperature Sensors .....                                          | 11 |
| Hydrologic Matric Potential Sensors .....                          | 11 |
| CHEMICAL SENSOR FIELD DEMONSTRATIONS .....                         | 15 |
| Adsistors™ .....                                                   | 16 |
| Gore-Sorbers .....                                                 | 18 |
| Litmus Paper .....                                                 | 23 |
| Dräger Tubes .....                                                 | 23 |
| PORTABLE AND/OR AUTOMATED GAS ANALYZER DEMONSTRATIONS .....        | 25 |
| ULTRAVIOLET FLUOROMETER MEASUREMENTS .....                         | 29 |
| ASSESSMENT OF SOIL VAPOR MOVEMENT DUE TO BAROMETRIC PUMPING .....  | 31 |
| Background .....                                                   | 31 |
| Vapor Movement Test .....                                          | 33 |
| Net Soil Gas Displacement .....                                    | 36 |
| Inferring Vertical Permeability with Transient Pressure Data ..... | 40 |
| OTHER SUPPORT ACTIVITIES .....                                     | 51 |
| SUMMARY AND RECOMMENDATIONS .....                                  | 53 |
| REFERENCES .....                                                   | 57 |
| APPENDIX A .....                                                   | 58 |

## LIST OF FIGURES

|                                                                                                                    |    |
|--------------------------------------------------------------------------------------------------------------------|----|
| 1. SEAMIST™ deployment system .....                                                                                | 4  |
| 2. General location of the SNL CWL. The unlined chromic acid pit is in the lower southwest corner of the CWL ..... | 6  |
| 3. Location of UCAP boreholes in the CWL .....                                                                     | 7  |
| 4. Pressure scanning and data recording systems used to monitor in-situ soil gas pressures .....                   | 10 |
| 5. Comparison between downhole temperature histories measured with a PRT and a type K thermocouple .....           | 12 |

|                                                                                                                                                                 |    |
|-----------------------------------------------------------------------------------------------------------------------------------------------------------------|----|
| 6. Matric potential histories recorded during the second test (a) at 6 feet bgs, and (b) at 51 feet bgs .....                                                   | 13 |
| 7. Laboratory test results showing normalized Adsistor™ resistance change to 100 ppm TCE in air .....                                                           | 17 |
| 8. Field measurements showing transient response of Adsistors™ .....                                                                                            | 17 |
| 9. Example of the change in Adsistor™ response for all elevations .....                                                                                         | 19 |
| 10. Profile of detected amounts of 1,1,1-TCA using Gore-Sorbers .....                                                                                           | 21 |
| 11. Profile of detected amounts of TCE using Gore-Sorbers .....                                                                                                 | 21 |
| 12. Profile of detected amounts of PCE using Gore-Sorbers .....                                                                                                 | 21 |
| 13. Profile of detected amounts of 1,2-DCB using Gore-Sorbers .....                                                                                             | 21 |
| 14. Profile of detected amounts of Acetone using Gore-Sorbers .....                                                                                             | 22 |
| 15. Profile of detected amounts of Pentane using Gore-Sorbers .....                                                                                             | 22 |
| 16. Profile of detected amounts of Freon using Gore-Sorbers .....                                                                                               | 22 |
| 17. Profile of TCE concentration detected using Dräger tubes with SEAMIST™ gas withdrawal ports .....                                                           | 24 |
| 18. Contaminant histories from automated GC analysis of soil gas drawn from SEAMIST™ sampling tubing .....                                                      | 27 |
| 19. Schematic diagram of ultraviolet fluorometer .....                                                                                                          | 29 |
| 20. Comparison of surface barometric pressure with pressure at depth for UCAP3 .....                                                                            | 32 |
| 21. Simplified model of the effect of barometric pressure on soil vapor movement at depth .....                                                                 | 32 |
| 22. Plan view of the UCAP, TEVES, and GeoProbe installations .....                                                                                              | 34 |
| 23. Three-dimensional layout of the UCAP boreholes .....                                                                                                        | 35 |
| 24. Permeability measurement results for the TEVES boreholes .....                                                                                              | 37 |
| 25. Permeability measurement results for the UCAP boreholes .....                                                                                               | 38 |
| 26. Pressure history versus depth for UCAP3 .....                                                                                                               | 39 |
| 27. Comparison of pressure responses from SEAMIST™ pressure ports and Geoprobe ports at depths with atmospheric pressure and soil gas pressure at 95 feet ..... | 39 |
| 28. Calculational sequence to determine vapor displacement: a) recorded pressure data, b) pressure difference, c) gas velocity, and d) displacement .....       | 41 |
| 29. Displacement calculations for UCAP1 .....                                                                                                                   | 42 |
| 30. Displacement calculations for UCAP2 .....                                                                                                                   | 43 |
| 31. Displacement calculations for UCAP3 .....                                                                                                                   | 44 |
| 32. Time series analysis sequence to determine amplitude ratio between the surface pressure and the soil gas pressure at 95 -foot depth .....                   | 46 |
| 33. Relationship between Fourier modulus and amplitude ratio .....                                                                                              | 47 |
| 34. Resulting estimated permeabilities derived from the time series analysis (UCAP and Geoprobe measurement points) .....                                       | 49 |
| 35. Schematic representation of the SEAMIST™ system installed beneath the KAFB RB -11 landfill .....                                                            | 51 |

## LIST OF TABLES

|                                                                                                |    |
|------------------------------------------------------------------------------------------------|----|
| 1. Summary of the chemical sensors on the SEAMIST™ membrane placed in the UCAP3 borehole ..... | 15 |
| 2. Gore-Sorber target compound summary (units are $\mu\text{g}/\text{sorbent module}$ ) .....  | 20 |
| 3. Summary (average) concentration results .....                                               | 26 |
| 4. Calculated porosity of the split spoon samples from the UCAP boreholes .....                | 48 |

## ACRONYMS

|           |                                                   |
|-----------|---------------------------------------------------|
| bgs       | below ground surface                              |
| CWL       | Chemical Waste Landfill                           |
| DOE       | Department of Energy                              |
| FFT       | Fast Fourier Transform                            |
| GC        | gas chromatograph                                 |
| ID        | inside diameter                                   |
| IUPAC     | International Union of Pure and Applied Chemistry |
| MEK       | Methyl Ethyl Ketone                               |
| MWL       | mixed waste landfill                              |
| MWLID     | Mixed Waste Landfill Integrated Demonstration     |
| OD        | outside diameter                                  |
| PCE       | Penta chloroethane                                |
| PRT       | platinum resistance thermometer                   |
| SEA       | Sciences and Engineering Associates, Inc.         |
| SNL       | Sandia National Laboratories                      |
| T         | n-pentane                                         |
| TCE       | Trichloroethylene                                 |
| TCP       | thermocouple psychrometer                         |
| TetCe     | tetrachloroethylene                               |
| TEVES     | Thermally Enhanced Vapor Extraction System        |
| UCAP      | unlined chromic acid pit                          |
| VOC       | volatile organic compound                         |
| 1,2, DCB  | 1,2, Dichlorobenzene                              |
| 1,1,1 TCA | 1,1,1 Trichloroethane                             |

**Intentionally Left Blank**

## INTRODUCTION

The Mixed Waste Landfill Integrated Demonstration (MWLID) was tasked with demonstrating innovative technologies for the cleanup of chemical and mixed waste landfills that are representative of sites occurring throughout the Department of Energy (DOE) complex and the nation. Characterization and remediation at the MWLID emphasize in-situ technologies that promise to reduce the risk to the environment and personnel, save time, and produce more complete descriptions of underground processes. The MWLID focused on two landfills located in Area III at Sandia National Laboratories (SNL) on Kirtland Air Force Base in Albuquerque, New Mexico: the Chemical Waste Landfill (CWL) and the Mixed Waste Landfill (MWL).

The 1.9-acre CWL was operated from 1962 to 1985; during this time a wide variety of organic and inorganic chemicals were disposed of at the site. About 450,000 cubic feet of contaminated material are believed to be in the CWL, including oxidizers, reducers, solvents and other organics, acids and alkali, and heavy metals.

The 1.6-acre MWL received hazardous and radioactive waste from 1959 to 1962, after which it received only radioactive waste (including classified radioactive waste) until its closing in 1988. Soil borings taken in 1989 indicate elevated tritium concentrations up to 100 feet beneath the MWL.

Both the CWL and the MWL are situated in alluvial deposits of alternating clays, sands, and gravels approximately 12,000 feet thick. A complex fault system controls ground water flow and, in some cases, the hydraulic connection across the faults is unknown. The aquifer below the landfills is believed to be over 10,000 feet thick, with the top of the aquifer lying approximately 500 feet below the surface. The arid Albuquerque climate receives, on average, less than eight inches of precipitation annually. The potential evapotranspiration rate is very high, with a natural recharge rate that is only a few percent of the precipitation rate.

Characterization and monitoring needs exist at both the CWL and the MWL. To address these needs the MWLID used the SEAMIST™ system, an instrumentation and fluid sampler emplacement technique designed for in-situ characterization and monitoring. This system was developed by Science and Engineering Associates, Inc., (SEA) with DOE (Argonne National Laboratory) support explicitly to address DOE unsaturated zone characterization and monitoring needs. Since 1992, SEAMIST™ systems have been used in characterization and monitoring demonstrations in the CWL. Activities described here include laboratory-scale and field evaluation of in-situ vadose zone sensors and samplers integrated with the SEAMIST™ deployment system. These include thermocouple psychrometers, gypsum blocks, pressure transducers, temperature sensors, colorimetric indicators, and hydrocarbon-sensitive adsorbing resistors. Using SEAMIST™, these sensors were successfully emplaced and operated in the CWL unlined chromic acid pit (UCAP) boreholes. These tests have demonstrated the capability of measuring detailed pressure gradients and high resolution temperature and matric potential parameters. Standard SEAMIST™ vapor sampling systems were also integrated with state-of-the-art volatile organic compound (VOC) analysis technologies (e.g., automated gas chromatograph and ultraviolet laser fluorometer).

**Intentionally Left Blank**

## INTEGRATING SENSORS WITH SEAMIST™

The SEAMIST™ system utilizes an inverting, pneumatically deployed tubular membrane to deploy sensors and sampling devices in boreholes. Figure 1 illustrates the deployment technique. Depending on the sensor requirements, the sampling devices can be mounted on the interior or exterior of the membrane. Signal cables or tubing are typically run to the surface on the inside of the membrane. Pressure-tight feedthroughs allow the cable or tubing to pass through the membranes and basepipe without damaging the system's pressure integrity.

The basic requirement for any sensor emplaced with SEAMIST™ is that the sensor and its data cable are not damaged by the membrane emplacement process and the membrane is not damaged by the sensor hardware. Consequently, the cable (electrical or fiber optic) must be flexible and strong enough to withstand the membrane's inversion process, which will subject it to a worst-case bend radius of one quarter of the borehole diameter. For maximum ease of emplacement, the detector or sampler should be no longer (in its dimension along the borehole axis) than half the borehole diameter. However, if a sensor's cabling is very flexible and the sensor itself is fairly rugged, it is possible to deploy a sensor whose longitudinal dimension is just less than the borehole diameter. About two thirds of the SEAMIST™ installations to date have been in 8- to 12-inch diameter boreholes, with the balance in roughly 4-inch-diameter casings or directionally drilled holes. All of the instruments tested for the MWLID easily satisfy the physical emplacement requirements.

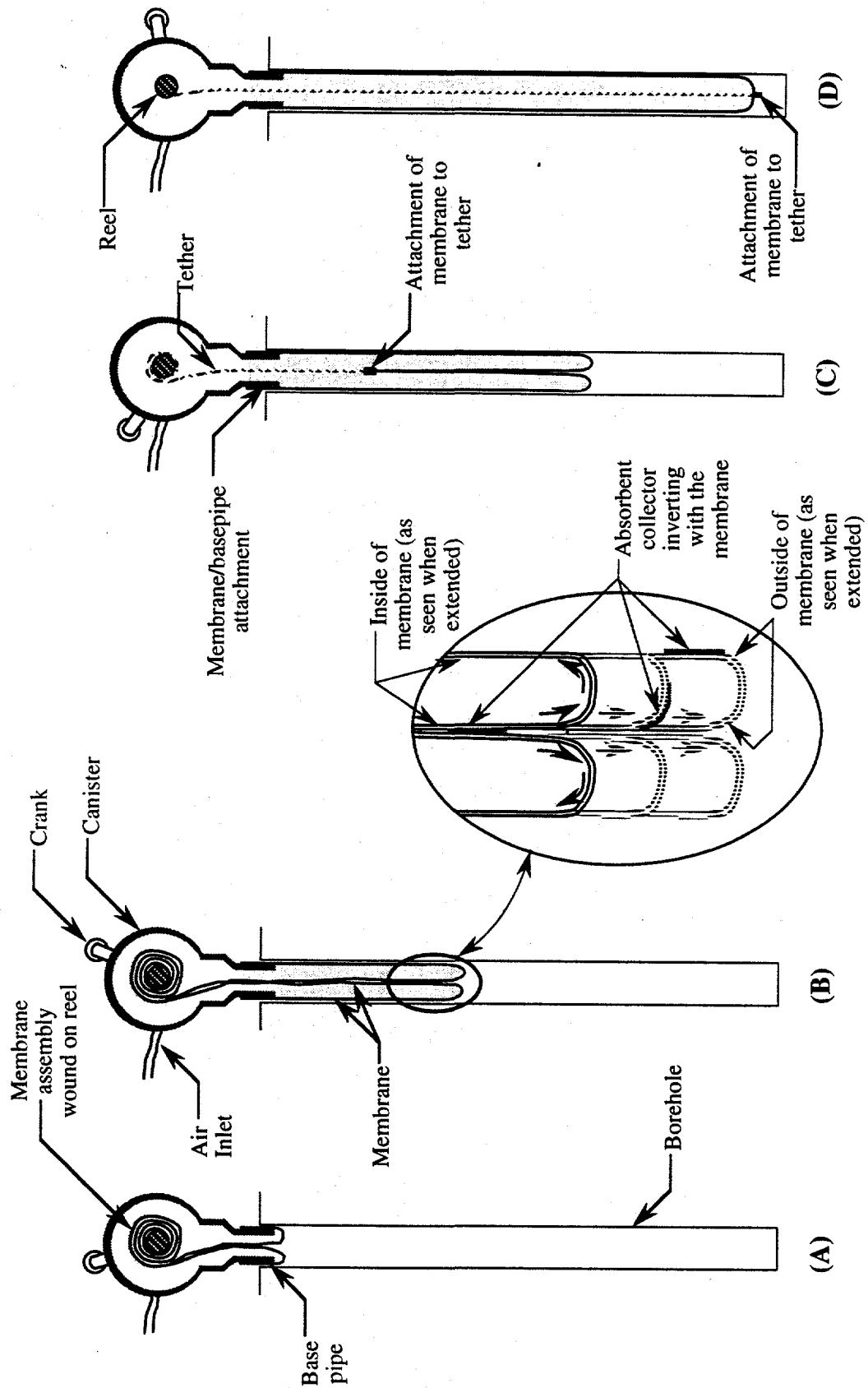


Figure 1. SEAMIST™ deployment system.

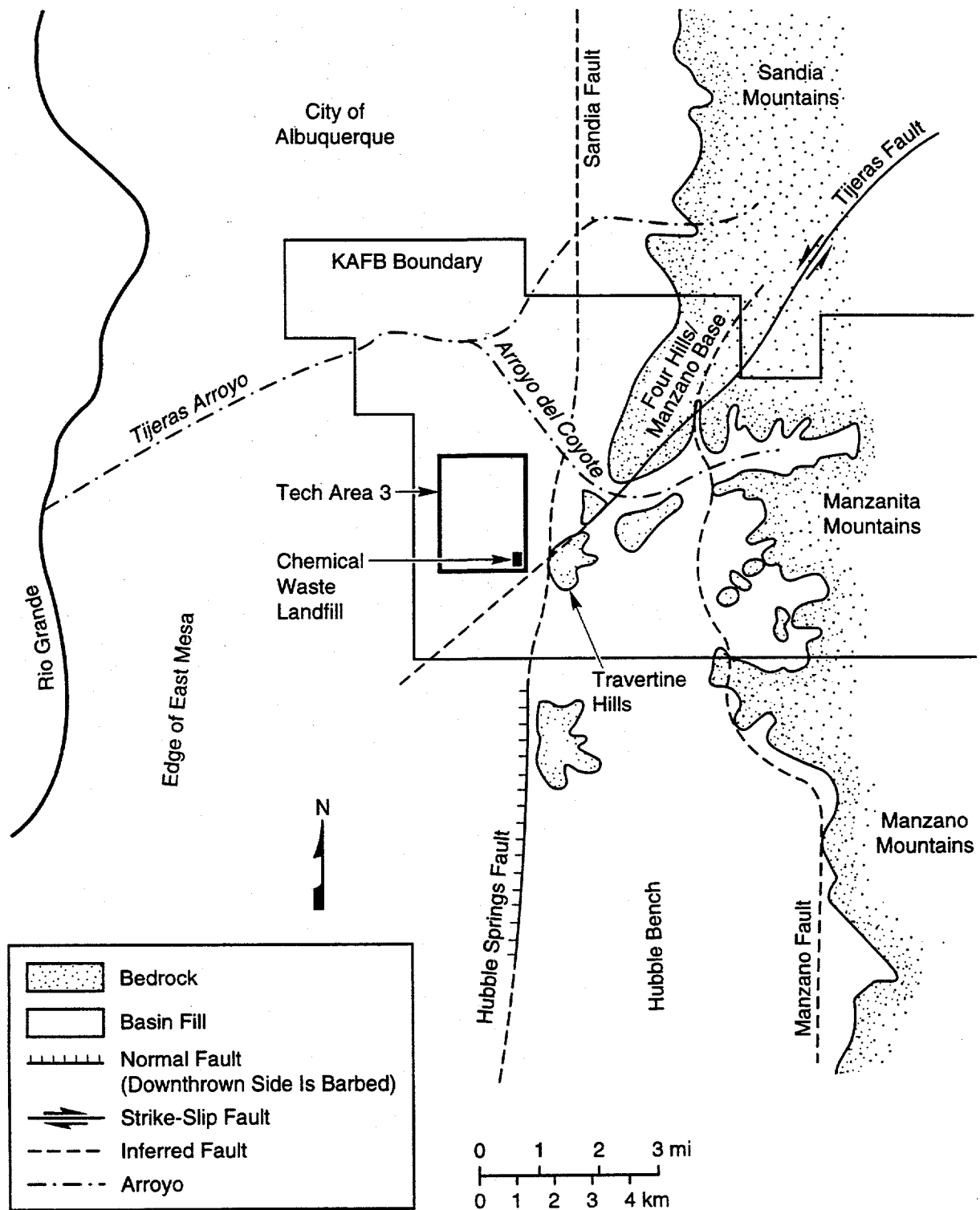
## GENERAL DESCRIPTION OF THE EXPERIMENT SETTING

The CWL is located in Sandia's Technical Area III (Figure 2). The landfill was created in 1962 to accept waste chemicals generated by SNL. It was designed to segregate incoming wastes by chemical group to minimize any adverse chemical reactions. Individual disposal pits were excavated for each chemical group. Typically, these pits were small, about 15 feet wide by 45 feet long by 15 feet deep, although larger trenches were created to contain large objects. The disposal cells were generally not lined, and the soils were not amended to alter the natural soil texture.

A chemical waste disposal ticket system was used to track waste picked up from SNL facilities until its disposal at the CWL. Disposal tickets for the period from 1975 to 1982 were evaluated for the types and quantities of waste disposed into the waste group disposal pits. Because all waste groups were given the same identification number, the quantity of waste disposed at a particular location can only be crudely estimated. A wide variety of chemical wastes was disposed, including many VOCs.

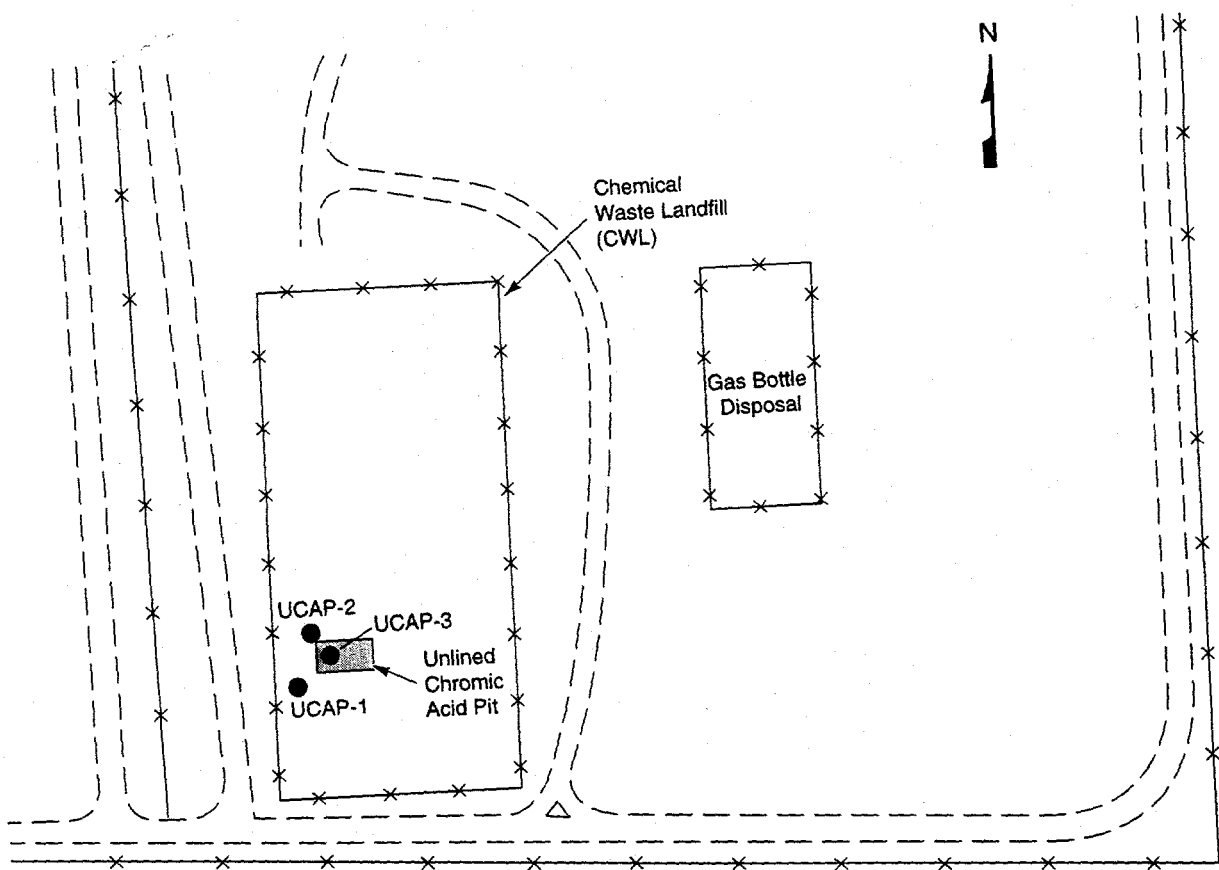
Three wells were bored in or near the UCAP for characterization and monitoring purposes (Figure 3). The wells designated UCAP1, UCAP2, and UCAP3 were drilled using a truck-mounted Drill Systems/Link-Belt AP-1000 dual-tube percussion drilling rig equipped with 9-inch-OD casing and 10-inch-OD bit (IT Corporation, 1992). Soil samples from each boring were collected at 5-foot intervals with a 2 1/2-inch ID- by 24-inch long California split-spoon sampler. All borings were drilled to a total depth of 125 feet below ground surface (bgs). Caliper logs of the wells showed numerous washed-out regions in each of the wells, with the diameters ranging from the nominal bit outside diameter (OD) of 9.25 inches to almost 18 inches. Depths of 106, 96, and 102 feet were recorded for UCAP1, UCAP2, and UCAP3, respectively. Each well was sealed using an uninstrumented SEAMIST™ liner. The SEAMIST™ systems remained in the wells until in-situ instrument demonstrations were completed in the summer of 1992.

The liners were removed in December 1992 to allow open borehole anemometry and gas permeability measurements (which were completed by the end of January 1993).



TRI-6621-30-0

Figure 2. General location of the SNL CWL. The unlined chromic acid pit is in the lower southwest corner of the CWL.



TRI-6621-22-1

Figure 3. Location of UCAP boreholes in the CWL (Ref. 3).

**Intentionally Left Blank**

## PHYSICAL PROCESS SENSOR FIELD DEMONSTRATIONS

Numerous sensors for characterizing the downhole in-situ environment were incorporated with the SEAMIST™ deployment system for the field tests. These sensors included small absolute pressure transducers and pressure ports that can measure in-situ pressures, high precision platinum resistance thermometers that can precisely measure in-situ temperatures, and several devices (thermocouple psychrometers, gypsum blocks, and relative humidity sensors) that can measure the matric potential in-situ. All sensors were monitored with a Campbell Scientific CR7 datalogger. The CR7 was used to control the frequency of data collection, convert raw output values to engineering units, and record and store all data. A photovoltaic system capable of a 0.5-Amp continuous load supplied power to the solenoid valves and Vaisala pressure transducer used to measure atmospheric, membrane, and downhole port pressures and to the DC pumps that pressurized the membranes. The photovoltaic system was also used to trickle charge the CR7. Figure 4 shows the general setup of the field experiments.

The SEAMIST™ membrane used to field test the physical process sensors was fabricated from a lightweight (4.5 ounces per square yard) urethane-coated polyester fabric. All the sensor cables except those for the gypsum blocks were run into a feedthrough in the basepipe inside the membrane (enclosed in a fabric pocket) and to the desired sampling location. Sensors and cabling were passed through the membrane to the soil side via airtight feedthroughs. Strips of material welded over the sensor cabling near the sensors held the units firmly in place. Cabling from the gypsum blocks was run down the outside of the membrane (also in an enclosed pocket) because potted capacitors in the cabling were too large to pass through the airtight feedthroughs. The gypsum blocks were attached to the membrane using a 6-inch-diameter cork disk backing assembly, which pressed the block's bottom surface directly into the soil.

Sampling elevations of 6 and 51 feet bgs were chosen for sensor installation. These elevations correspond to depths where permeability, soil pressure history measurements, and/or gas chromatograph analysis data were available. Locations were also chosen to yield representative data under both deep and near surface conditions. Each sensor type was included at each elevation, staggered over a 1-foot interval along the membrane's diameter. A coarse weave mesh covered the sensors (except the gypsum block) to ensure the sensors would be in contact with the soil gas.

The SEAMIST™ sensor system was used in UCAP2 for two field test sequences. The first sequence included emplacement, data collection at one-half hour intervals for 120 hours, and retrieval. In between the field test sequences, the SEAMIST™ sensor system was removed and a system check was conducted. At this time it was noted that the relative humidity sensor at the 6-foot elevation was not responding as expected. The membrane was redeployed and data collection set at 1-hour intervals. At approximately 24 hours, the membrane was deflated and a replacement relative humidity sensor was installed at the 6-foot elevation. Data collection was not halted during this time. The membrane was reinflated and data were collected for an additional 112 hours. The DC pump used to maintain the membrane's pressure failed during this field test sequence, and the membrane's overpressure decayed from slightly above 1 psi to 0 psi over 10 hours. The effect of the pressurized system varied from sensor to sensor and will be discussed in the results sections.

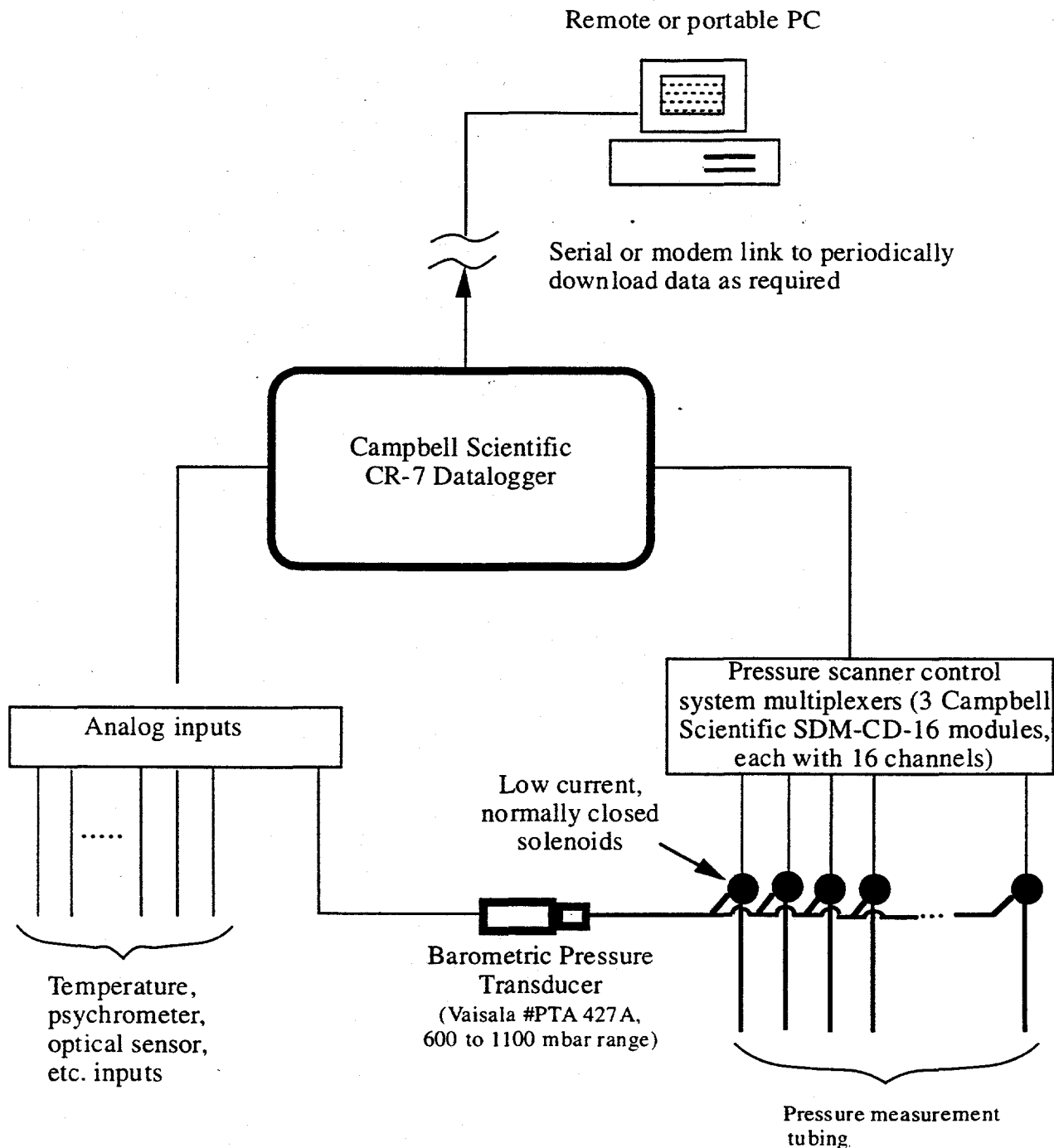


Figure 4. Pressure scanning and data recording systems used to monitor in-situ soil gas pressures.

## Pressure Sensors

Soil gas pressure measurements can be conducted with the SEAMIST™ system by either locating the pressure transducer on the surface or downhole. The surface-located method requires that a small diameter tube be run from the pressure transducer to the desired sensing elevation. Alternatively, the pressure transducer can be emplaced downhole with a cable running from the transducer to a recording device at the surface. For comparison, each method was included in the field demonstration. Instrumentation used with the first method included a PTA 427A Vaisala pressure transmitter connected to a manifold which could switch between any of several 1/8-inch OD, 1/16-inch ID tubes (Figure 4). The atmospheric pressure, membrane pressure, and sampling-elevation pressures were measured with this gauge. The second method of measurement was conducted by locating a calibrated and temperature-compensated Motorola model MPX5100 absolute pressure sensor at each sampling location. The Motorola sensors were calibrated to the Vaisala transducer in the laboratory prior to deployment; thus the only anticipated variance in the data was an offset caused by the difference in elevation of the transducers, an offset of 0.22 and 1.85 mbar for the 6- and 51-foot elevations, respectively.

Both techniques for measuring in-situ soil gas pressure were easily integrated with the SEAMIST™ system. Each method had both advantages and drawbacks. The advantages of the surface-located pressure transducer include its abilities to measure multiple sample elevations with a single high precision transducer and to easily reuse the transducer with different SEAMIST™ systems. The drawback with the transmitter was its temperature sensitivity when conducting very precise soil gas measurements. This sensitivity can be minimized either by insulating the transducer to minimize temperature fluctuations or by using a transducer compensated to a wide temperature range.

Placing the pressure transducer in the borehole at the desired elevation is necessary when very rapid pressure measurements are desired compared to the sampling depths desired. The offset drift seen in the Motorola gauges would render them unusable for long term high precision monitoring applications, but a gauge with higher precision could easily be used.

## Temperature Sensors

Most temperature sensors are of a size and configuration convenient for SEAMIST™ deployments. For this field experiment, a high-precision platinum resistance thermometer (PRT) and a type K thermocouple were used. The PRT was chosen because of its precision and accuracy. Very precise temperature measurements are necessary, for example, when performing soil moisture flux measurements near the surface.

To illustrate the different accuracies of a PRT and a thermocouple, Figure 5 shows the plots of the histories of the two devices recorded at the same depth (6 feet) over the same time. The PRT was attached to the SEAMIST™ system in UCAP2, and the thermocouple was attached to a SEAMIST™ system in UCAP3, approximately 17 feet away. The PRT is the more stable of the two devices and yields more precise measurements. This may be due to the sensitivity of the thermocouple measurement to temperature gradients inside the datalogger, which impact its cold junction reference.

## Hydrologic Matric Potential Sensors

Three different devices for measuring hydrologic matric potential were field tested: a soil moisture block, thermocouple psychrometer (TCP), and resistive relative humidity sensors.

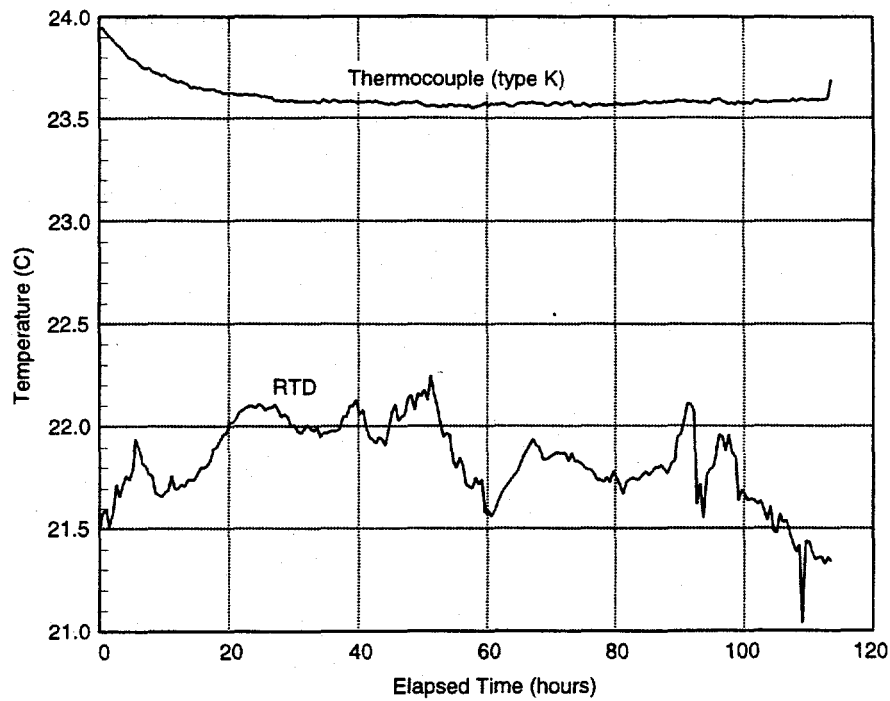
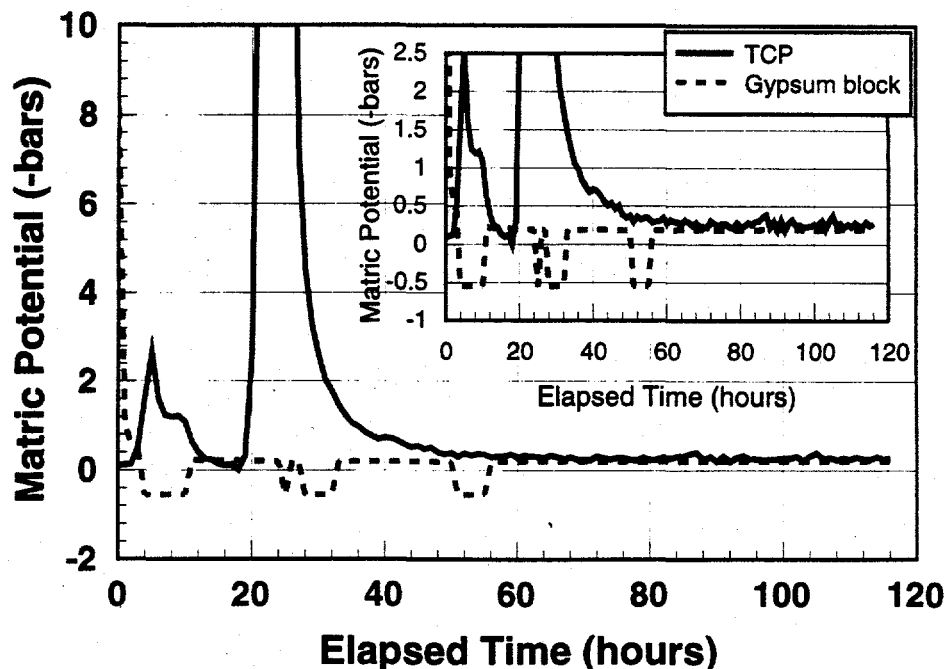


Figure 5. Comparison between downhole temperature histories measured with a PRT and a type K thermocouple. Data were collected during the first test at 6 feet bgs.

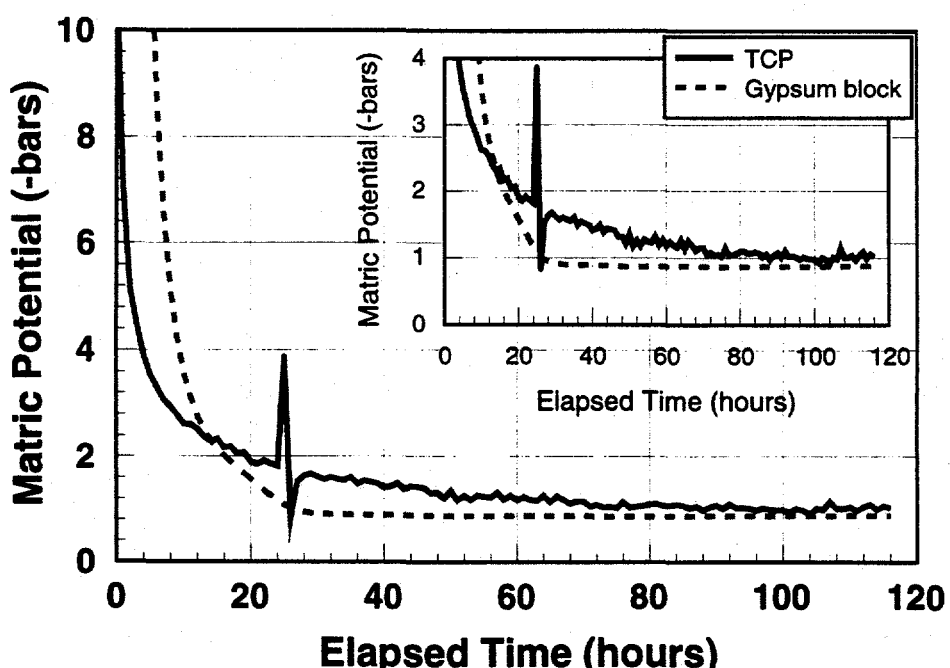
A soil moisture block measures the matric potential by equilibrating the capillary tension in a porous block in contact with the soil. The moisture content of the porous block is then determined by an electrical resistance measurement. For this test, a Delmhorst model 227 soil moisture gypsum block with a -0.1 to -10 bar range was chosen. TCPs and relative humidity sensors measure hydrologic matric potential by calculating the relative humidity of the soil vapor, which is related to the soil water capillary tension. A WESCOR model PST-55 TCP was chosen because it can accurately measure matric potential between -1 and -70 bars; however, it is less accurate in the 0 to -1 bar range. In very dry soils with matric potentials less than -70 bar, a relative humidity sensor can be used to measure the soil's relative humidity. The sensor chosen for testing, an Ohmic MHS series, is capable of measuring relative humidity between 80 and 99 percent (-300 to -10 bars, approximately).

The SEAMIST™ membrane was deployed in UCAP2 and data were collected for 120 hours. For this test, both the gypsum blocks were deployed in a partially saturated condition (~1cc of water was absorbed by each block prior to emplacement) to decrease the time required to equilibrate.

Results from the 6-foot sampling location show the gypsum block absorbed moisture from the surrounding soil very rapidly (< 12 hours) and equilibrated at -0.2 bars (Figure 6). The equilibration of the gypsum block is highly dependent on its saturation state when deployed. The equilibrated thermocouple psychrometer reading of -0.3 bars was very close to that



(A)



(B)

Figure 6. Matric potential histories recorded during the second test (a) at 6 feet bgs, and (b) at 51 feet bgs.

measured by the gypsum block. This corresponds to a moisture content of 19 to 28 percent. The depressurization of the membrane, to insert a replacement relative humidity sensor (~24 hours into the test), is clearly depicted in the TCP history, but unnoticeable in the values recorded with the gypsum block (Figure 6). The relative humidity sensor at this sampling location read out of range.

Sensors located at the 51-foot sampling elevation responded similarly to those at the 6-foot elevation. The gypsum block equilibrated approximately 30 hours after deployment to a -0.9 bar matric potential reading. The TCP equilibrated to a very similar matric potential value of -1.0 bars within 72 hours of deployment. This is equivalent to a moisture content of 5 to 20 percent. Again, the TCP detected the time when the system was deflated to insert the relative humidity sensor. The response of the depressurization was not as pronounced as it was in the 6-foot sampling record because the effect of the depressurization was not as great at the lower depth. The relative humidity sensor recorded a varying but generally decreasing matric potential to -2 bars until, after 78 hours, the sensor began reading out of range.

Although no prior in-situ hydrologic matric potential analysis has been performed at the UCAP, laboratory analysis of physical and hydraulic properties on soil samples collected from numerous boreholes drilled in this area have been conducted. Two of the laboratory tests included measuring the initial moisture content and moisture characteristics of the samples. Complete analysis techniques and results can be found in (Stephens, 1989). The moisture content reported by Daniel B. Stephens & Associates, Inc. for a depth of 6 feet was 3 to 7 percent, which is 16 to 21 percent lower than that determined using the SEAMIST™ sensor system. The reported moisture content at 51 feet was similarly lower than that determined in situ. This might be an artifact of in-situ versus ex-situ measurements.

All the hydrologic matric potentials sensors were easily deployed with the SEAMIST™ system. They yielded results that were both reproducible and consistent from sensor type to sensor type, with the exception of the relative humidity sensor, which could not measure in this range. The time required to reach equilibrium was long (12 to 72 hours or longer) for all the sensors.

## CHEMICAL SENSOR FIELD DEMONSTRATIONS

Several chemical sensors that show promise for vadose-zone monitoring were also incorporated with the SEAMIST™ system. The following sensor types were placed into the UCAP3 borehole at the CWL using the SEAMIST™ system :

- Adsistors™ - adsorbent resistive sensors
- Gore-Sorbers - passive absorbent charcoal modules
- Dräger Tubes - colorimetric indicator tubes
- Litmus paper - pH indicating strips

The chemical sensors remained in the borehole for 288 hours. The primary purpose of the tests was to demonstrate and evaluate the compatibility of these sensors with the SEAMIST™ system. In addition, each sensor was evaluated for effectiveness of monitoring the vadose zone.

Chemical sensors were incorporated into a single SEAMIST™ membrane made from a urethane-coated polyester material. Table 1 shows the sensors attached to the SEAMIST™ membrane at each elevation. The membrane was 110 feet long with a diameter of 12 inches. Elevations of 6, 11, 18, 21, 31, 41, 51, 61, and 81 feet were chosen as data collection points. Gore-Sorbers and Adsistor™ sensors were placed at each of these elevations. In addition, a second Adsistor™ was placed at the 18-foot elevation for redundancy. Gas withdrawal ports were also located at each sensing location and connected to the surface by runs of Teflon® tubing. These ports served a dual function: They were used for ambient pressure measurement at each sensing point and as withdrawal lines for gas sample collection. Thermocouples were added to two of the locations to monitor temperatures.

Table 1. Summary of the chemical sensors on the SEAMIST™ membrane placed in the UCAP3 borehole.

| Elevation (ft) | Gas withdrawal port | Temperature probe | Adsistor™ ID | Gore-Sorber SN |
|----------------|---------------------|-------------------|--------------|----------------|
| 6              | ✓                   | ✓                 | 6            | 100877         |
| 11             | ✓                   |                   | 11           | 100876         |
| 18             | ✓                   | ✓                 | 18A & 18B    | 100875         |
| 21             | ✓                   |                   | 21           | 100874         |
| 31             | ✓                   |                   | 31           | 100873         |
| 41             | ✓                   |                   | 41           | 100872         |
| 51             | ✓                   |                   | 51           | 100871         |
| 61             | ✓                   |                   | 61           | 100870         |
| 81             | ✓                   |                   | 81           | 100869         |

Data were collected from the Adsistors™ and temperature probes on a Campbell Scientific CR7 data logger. Pressure measurements were also taken at each elevation by connecting the tubing run from each gas withdrawal port to a Vaisala barometric pressure transducer. Output from the pressure transducer was also recorded on the CR7. The litmus paper was tested separately. A length of the paper was lowered into the borehole and a SEAMIST™ membrane was deployed over it and pressurized to bring the paper into contact with the borehole wall.

### Adsistors™

Adsistors™ are simple absorbing sensors whose resistance changes as hydrocarbons are sorbed into the sensor. Although Adsistors™ presently are used to detect percent changes in hydrocarbon concentration, laboratory tests showed that they could sense hydrocarbon concentrations in the hundreds of ppm range (Figure 7). The SEAMIST™ membrane Adsistors™ system was emplaced in the UCAP3 borehole and monitored for 288 hours at an interval of 0.5 hours. Data were not collected from hour 113 to hour 188 because the CR7 was used for another experiment. The resistance of the Adsistor™ sensors was measured using a voltage divider measurement.

Each sensor is calibrated to determine its particular sensitivity constant and baseline resistance temperature variation. The resistance measured by the Adsistors™ can be related to gross hydrocarbon levels using sensitive constant and baseline resistance by:

$$c = k \log(R/R_0) \quad (1)$$

where:

$R$  = measured resistance ( $\Omega$ )

$R_0$  = baseline resistance ( $\Omega$ )

$c$  = contaminant concentration (ppm)

$k$  = sensitivity constant (ppm).

The Adsistors™ were not rigorously calibrated prior to field testing because the primary purpose of the tests was not to characterize the hydrocarbon contaminants in the CWL. However, to more accurately reflect relative hydrocarbon contaminant levels measured with the Adsistors™, some of the data obtained in the laboratory tests were used to reduce the raw data. This step was important because the relationship between resistance and concentration is  $R \propto 10^c$ . Relative changes in resistance values can be deceiving because they do not relate directly to hydrocarbon concentration levels.

The primary function of Adsistors™ as monitoring sensors is to detect changes in hydrocarbon concentration levels over time, particularly when the effectiveness of remediation activities is being monitored. To better illustrate this function, the data are normalized to values recorded at  $t=0$ . Plots of the normalized Adsistor™ data at elevations 6, 11, and 51 feet are shown in Figure 8.

On the day that the membrane was emplaced a weather front moved through the area. This resulted in a significant storm system residing in the area for several days. The drop in barometric pressure results in an upward displacement of soil gas, especially near the surface. This upward displacement of soil gas could account for the change in hydrocarbon contaminant

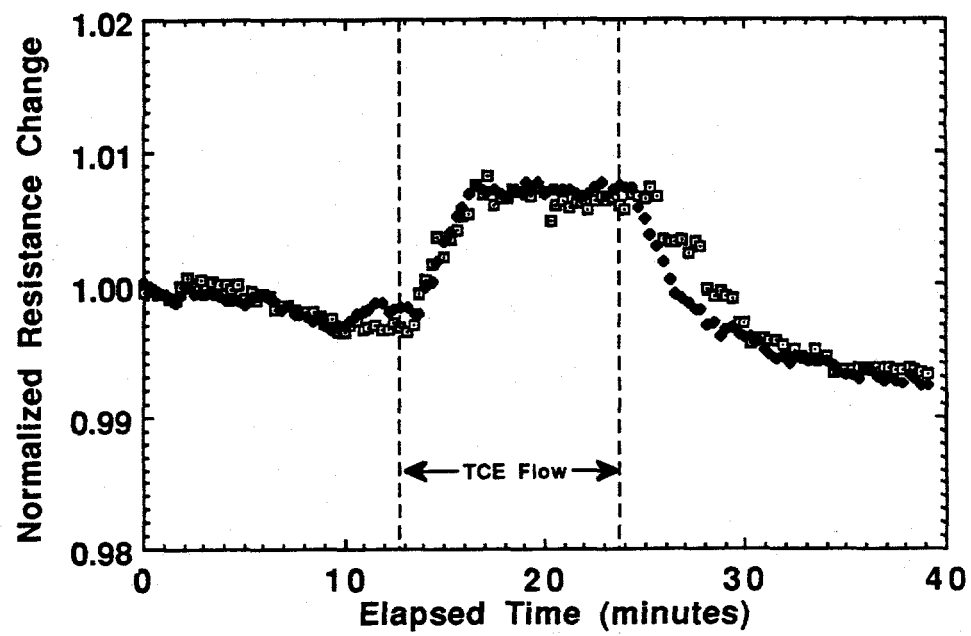


Figure 7. Laboratory test results showing normalized Adsistor™ resistance change to 100 ppm TCE in air.

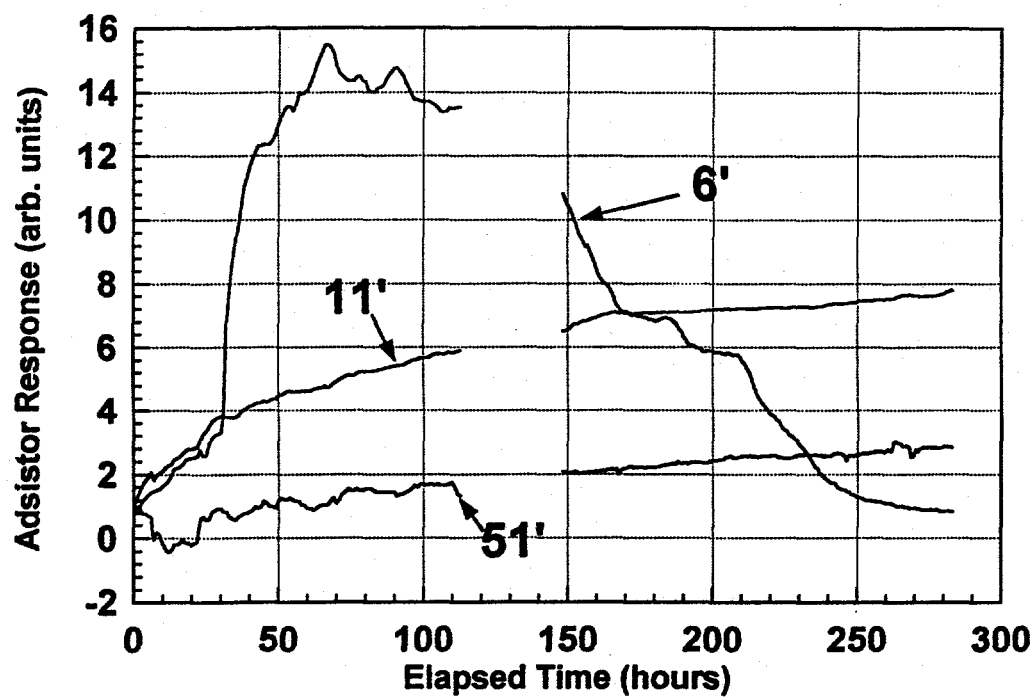


Figure 8. Field measurements showing transient response of Adsistors™.

concentration near the surface while little variation was noted at the depth. The disparity is shown in Figure 9, where the relative changes in hydrocarbon contaminant concentration from  $t=0$  for all elevations are plotted at the elapsed times of 67 and 250 hours.

Adsistors<sup>TM</sup> were easily incorporated with the SEAMIST<sup>TM</sup> system, and no deployment problems were encountered. Additional work is needed to refine this technology for use in monitoring applications. For example, the sensors must be housed in such a manner that their baseline resistances are not sensitive to sensor position. This problem is being addressed by the manufacturers of Adsistors<sup>TM</sup>, and prototype sensors are now available for testing. Furthermore, temperature compensation techniques must be used so that the sensitivity and baseline resistances of the sensor are not significantly affected by temperature. Temperature sensitivity must be a consideration if quantitative gas vapor concentration levels are to be determined with sensors.

### **Gore-Sorbers<sup>TM</sup>**

Gore-Sorbers<sup>TM</sup> are passive absorbent charcoal modules that can be placed within the SEAMIST<sup>TM</sup> membrane. These modules absorb contaminants that come in contact with the module. Analysis of a module shows the integrated amount of contaminants absorbed over the time the module is exposed to the contaminants. The Gore-Sorber<sup>TM</sup> modules were secured to the SEAMIST<sup>TM</sup> membrane by placing them in pockets made from nylon mesh, which were built onto the exterior of the membrane. As a control, a Gore-Sorber<sup>TM</sup> module was placed into an identical pocket secured to a swatch of membrane material and sealed in a glass container for the entire test period. The control was used to determine if the membrane material or pouch properties would affect the Gore-Sorber results.

The Gore-Sorbers<sup>TM</sup> were placed on the SEAMIST<sup>TM</sup> membrane approximately 31 hours prior to membrane emplacement in the UCAP3 borehole. The membrane was maintained at a pressure between 0.5 and 1.0 psi for the test period. At the end of the test period, the modules were removed from the SEAMIST<sup>TM</sup> membrane, placed in their respective shipping vials, sealed, and labeled. At this time the control sorber was also removed and placed in its vial. The vials were packed on ice and shipped by overnight delivery to W. L. Gore and Associates in Elkton, Maryland for analysis.

The Gore-Sorbers<sup>TM</sup> were analyzed for nine different compounds. Table 2 lists the concentrations of the target compounds found at each elevation. Values from the manufacturer's two controls and our controls are also given. The values found in the manufacturer's controls indicate the uncertainty in the measurements for each target compound. The values of the target compounds found in our control module fall within these uncertainties for all but toluene and 1,2 DCB. The level of 1,2 DCB found in the control is only of one significant digit. The materials used in the SEAMIST<sup>TM</sup> membrane did not contribute to detectable levels of 1,2 DCB. Small concentrations of toluene detected in the control module were comparable to the levels found in the modules exposed to the UCAP3 borehole wall. Analysis of a control module showed that the use of SEAMIST<sup>TM</sup> as a delivery vehicle for these sensors does not adversely affect their performance.

The Gore-Sorber analyses were graphed to better illustrate relative value differences of the compounds of a function of depth, (Figures 10 through 16). It should also be noted that the levels of TCE adsorbed by the modules at 41,61, and 81 feet saturated the modules and therefore are not representative of relative levels of TCE at these elevations in the UCAP3 borehole. The TCE concentration in the borehole far exceeds that of all other target contaminants. Graphs of toluene and MEK concentrations are not included because there was essentially no detection

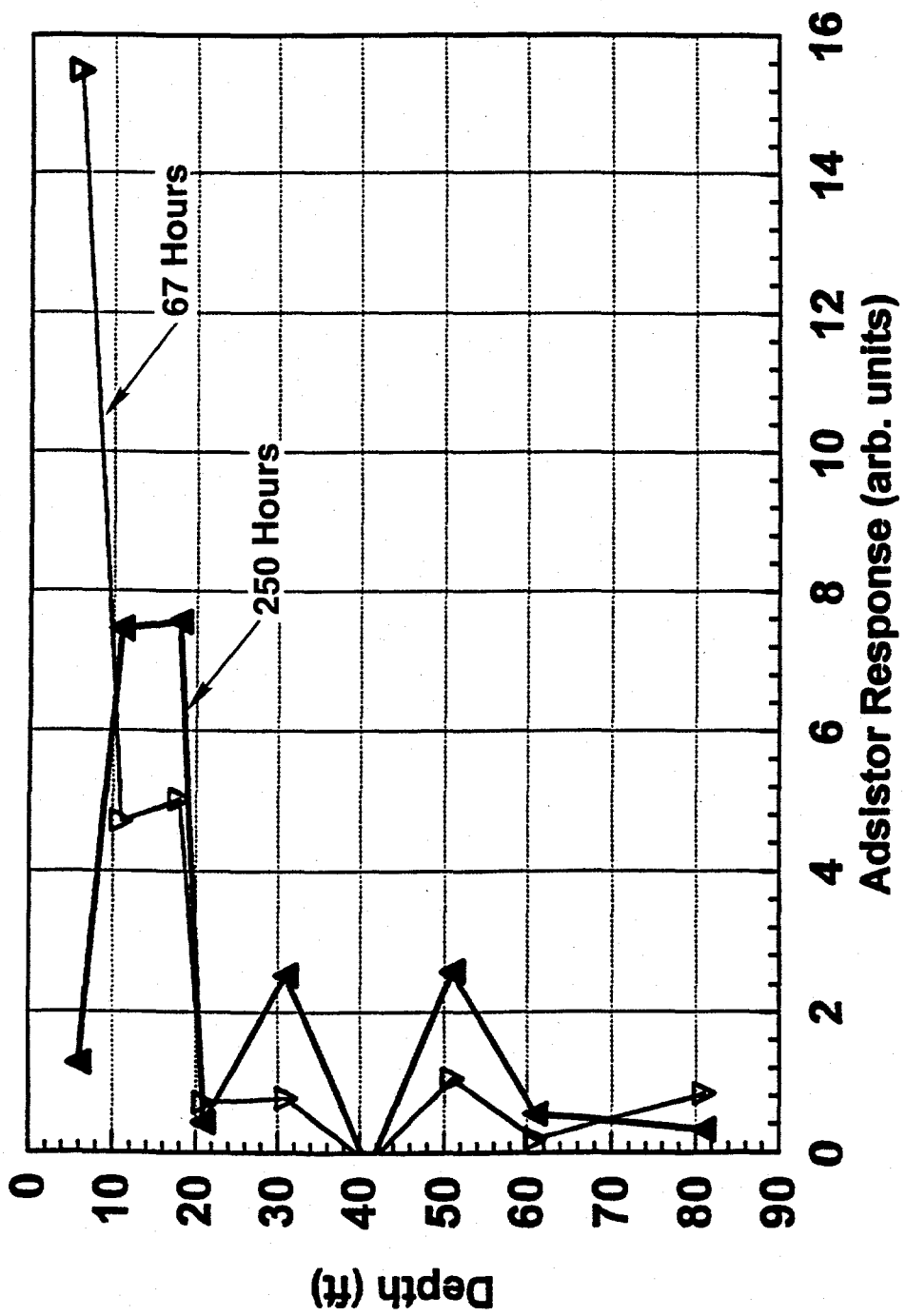


Figure 9. Example of the change in Adsistor™ response for all elevations. Data shown for elapsed times of 67 and 250 hours as normalized to initial values at t=0.

Table 2. Gore-Sorber target compound summary (units are  $\mu\text{g}/\text{sorbent module}$ )

| UCAP3 Elevation (ft) | Acetone ( $\mu\text{g}$ ) | Pentane ( $\mu\text{g}$ ) | Freon ( $\mu\text{g}$ ) | MEK ( $\mu\text{g}$ ) | 1,1,1-TCA ( $\mu\text{g}$ ) | TCE ( $\mu\text{g}$ ) | Toluene ( $\mu\text{g}$ ) | PCE ( $\mu\text{g}$ ) | 1,2-DCB ( $\mu\text{g}$ ) |
|----------------------|---------------------------|---------------------------|-------------------------|-----------------------|-----------------------------|-----------------------|---------------------------|-----------------------|---------------------------|
| 81                   | 0.8                       | 0.5                       | 13.5                    | 0                     | 57.41                       | >>1000                | 2.0                       | 40.6                  | 118.5                     |
| 61                   | 0.3                       | 0.4                       | 7.5                     | 0                     | 53.78                       | >>1000                | 2.1                       | 32.2                  | 100.2                     |
| 51                   | 0.2                       | 0.1                       | 13.5                    | 0                     | 57.94                       | 699                   | 1.6                       | 21.7                  | 108.0                     |
| 41                   | 0.1                       | 0.4                       | 7.5                     | 0                     | 38.86                       | >1000                 | 1.9                       | 27.3                  | 53.0                      |
| 31                   | 0.1                       | 0.4                       | 9.4                     | 0                     | 91.44                       | 674.34                | 1.4                       | 16.3                  | 69.9                      |
| 21                   | 0.0                       | 0.0                       | 0.0                     | 0                     | 36.19                       | 219.71                | 1.3                       | 9.4                   | 203.6                     |
| 18                   | 0.0                       | 0.0                       | 6.8                     | 0                     | 31.91                       | 156.76                | 1.2                       | 9.7                   | 5.0                       |
| 11                   | 0.3                       | 0.2                       | 0.2                     | 0                     | 0.79                        | 3                     | 1.2                       | 0.8                   | 70.4                      |
| 6                    | 2.3                       | 0.0                       | 0.5                     | 0                     | 0.38                        | 0.17                  | 1.2                       | 0.4                   | 98.2                      |
| control              | 0.1                       | 0.1                       | 0.1                     | 0                     | 0.06                        | 0                     | 1.1                       | 0.0                   | 0.1                       |
| mb1                  | 0.1                       | 0.2                       | 0.3                     | 0                     | 0.05                        | 0                     | 0                         | 0.0                   | 0.0                       |
| mb2                  | 0.0                       | 0.1                       | 0.2                     | 0                     | 0.07                        | 0                     | 0                         | 0.0                   | 0.0                       |

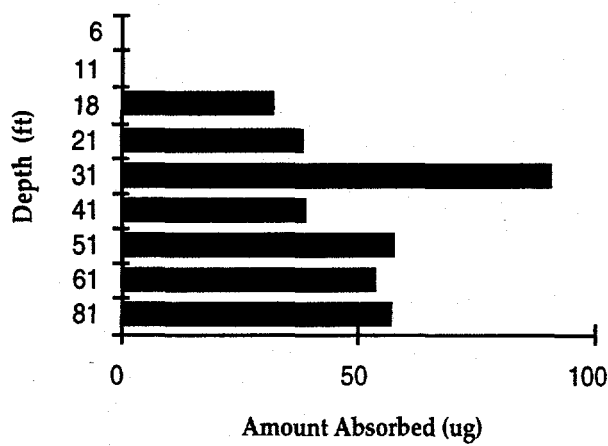


Figure 10. Profile of detected amounts of 1,1,1-TCA using Gore-Sorbers.

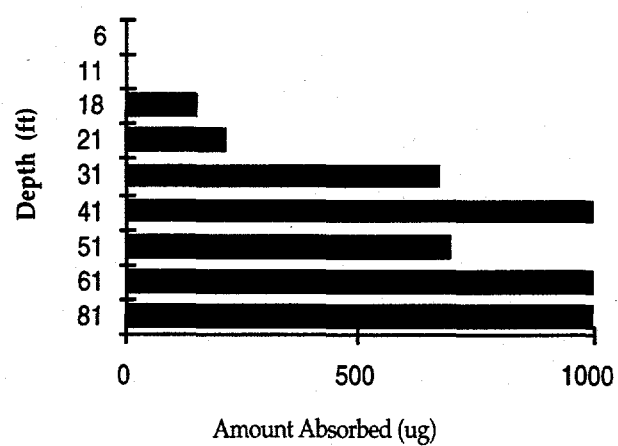


Figure 11. Profile of detected amounts of TCE using Gore-Sorbers.

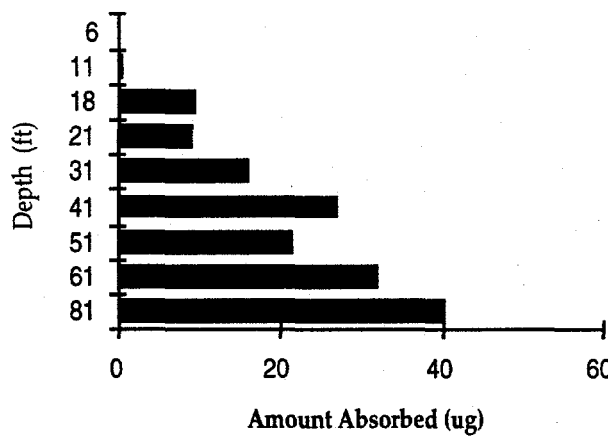


Figure 12. Profile of detected amounts of PCE using Gore-Sorbers.

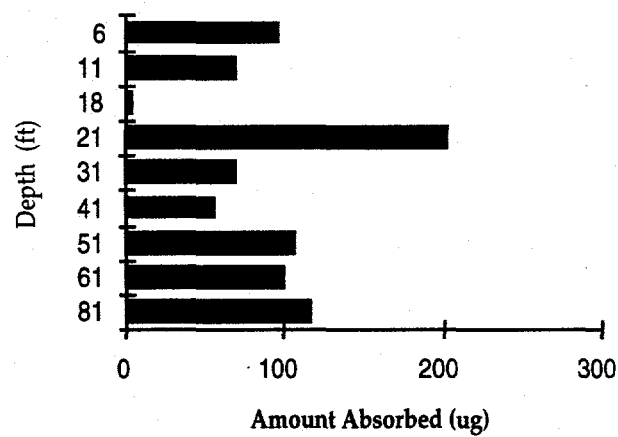


Figure 13. Profile of detected amounts of 1,2-DCB using Gore-Sorbers.

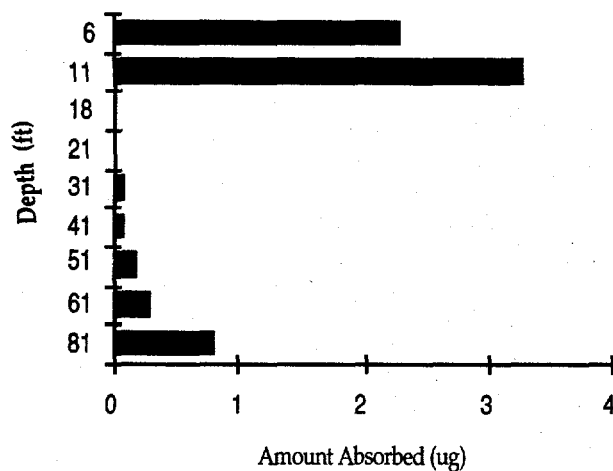


Figure 14. Profile of detected amounts of Acetone using Gore-Sorbers.

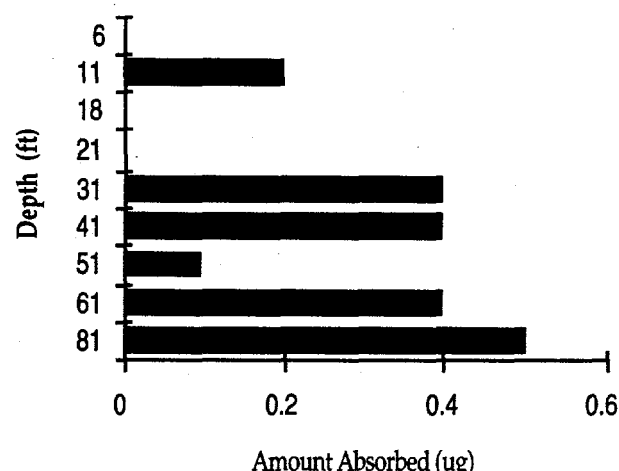


Figure 15. Profile of detected amounts of Pentane using Gore-Sorbers.

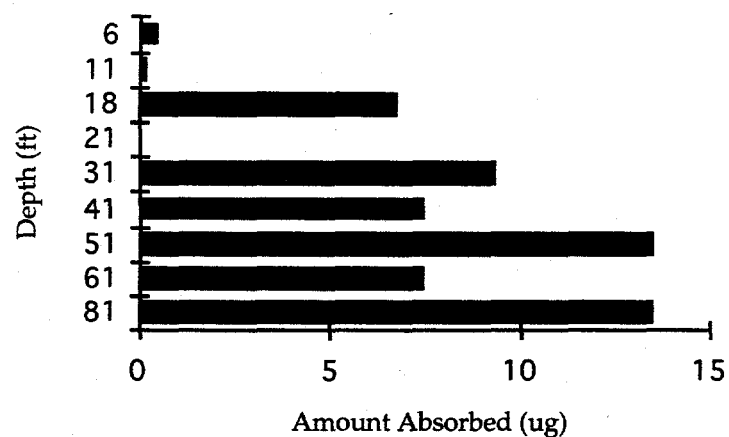


Figure 16. Profile of detected amounts of Freon using Gore-Sorbers.

of these compounds. Gore-Sorbers™ were readily incorporated by using mesh pockets mounted on the exterior of the SEAMIST™ membrane. The sorbers offered a high degree of precision with relatively simple handling procedures.

### **Litmus Paper**

Long lengths of litmus paper were used in an effort to determine the locations of chromic acid contamination in the UCAP3 borehole. The long strips (50 ft) were reinforced with nylon webbing and lowered into the borehole. Two duplicate strips were used. The litmus paper was then pressed firmly against the borehole wall using a pressurized SEAMIST™ membrane.

The major concern with this technique was whether the soil moisture would be adequate to wet the litmus paper; however, the paper began reacting after only 10 minutes. Unfortunately, the concentration of chromic acid was too low to be detected. The color indication showed nothing but the neutral value of the soil moisture. A possible remedy is to use pH paper with a much narrower range. The field test will be repeated using pH paper with ranges of 5.5 to 8.0 and 6.0 to 7.4. The fielding of this diagnostic technique is very fast and inexpensive.

### **Dräger Tubes**

Gas samples were taken from UCAP3 borehole using the SEAMIST™ membrane system for analysis with Dräger tubes. Tubes specifically sensitive to toluene and TCE were used. A minimum of two gas samples were taken at each test elevation: one each for the toluene-sensitive and TCE-sensitive tubes.

The Dräger tubes sensitive to toluene resulted in a non-detection at each elevation.

The results of the gas sampling conducted with tubes sensitive to TCE are shown in Figure 17, where the concentration of TCE noted in ppm is plotted at each elevation. Two distinct peaks in the TCE concentration are detected at the 31- and 51-foot elevations.

The use of Dräger tubes with SEAMIST™ gas withdrawal ports was successfully demonstrated. Sampling procedures required 5 to 10 minutes at each elevation with the bulk of the time used for filling the Tedlar bag. The material cost for collecting samples was on the order of \$5/sample. Given the short amount of time to obtain quantitative results and the low cost, the use of Dräger Tubes with the SEAMIST™ system offers a simple and cost effective technique for periodic monitoring and tracking and/or approximate contaminant gas concentrations in a borehole. Such a technique would be useful for tracking the effectiveness of remediation activities. The method could indicate appropriate times to analyze contaminant levels by accurate, more expensive analytical techniques such as gas chromatography.

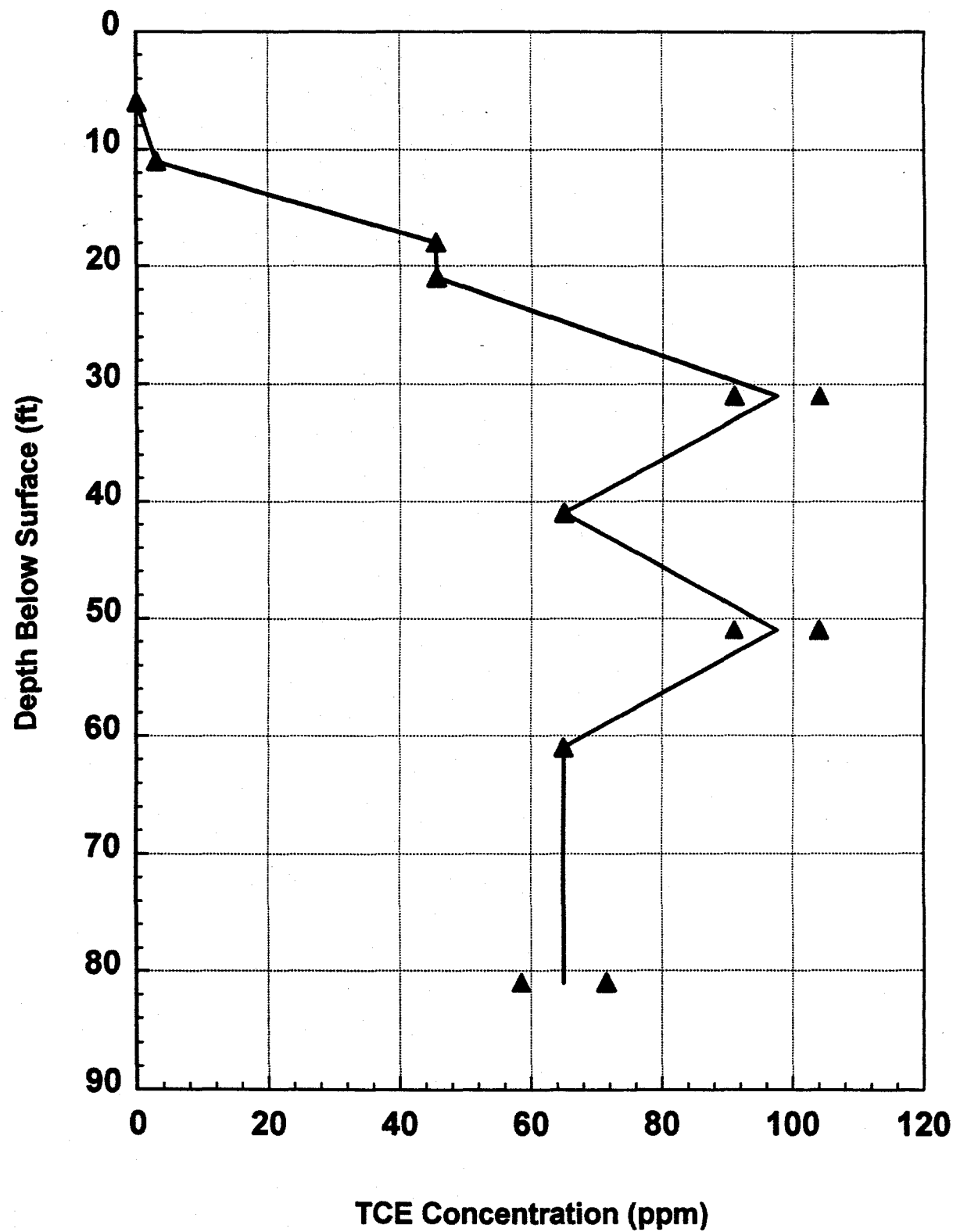


Figure 17. Profile of TCE concentration detected using Dräger tubes with SEAMIST™ gas withdrawal ports.

## **PORTABLE AND/OR AUTOMATED GAS ANALYZER DEMONSTRATIONS<sup>1</sup>**

The SEAMIST™ vapor sampling system was integrated with a modified, commercially available gas chromatograph (GC) and with an R&D ultraviolet imaging fluorometer to demonstrate its versatility and efficiency with a variety of instruments. Field tests of each integrated system were conducted at the CWL using the UCAP boreholes.

A commercially available GC was modified by SNL engineers for completely automated and unattended operation. The hardware modifications included: 1) attaching three vapor port sampling lines from the SEAMIST™ vapor sampling system to the multiport sampling valve on the GC and 2) adjusting the flow controller to a lower mass flow rate. The software modifications consisted of 1) changing the scheduling control file to four-run types instead of two-run types and 2) changing the main GC software control files to accommodate the altered timing necessary at the lower mass flow rate. The modified GC has been used on several other projects to detect VOCs. The GC has been calibrated to detect and quantify pentane, freon 113, 1,1,1-trichloroethane, trichlorethylene, toluene, tetrachlorethylene, ethyl benzene, o-xylene, and 1,2,-dichlorobenzene. A number of other compounds, including m-xylene and p-xylene, can be detected but not quantified.

A combined SEAMIST™/Automated GC test was conducted at the CWL site in Technical Area III. The goals were to detect, quantify, and monitor VOCs from three vapor ports at different depths (Port A at 6 feet, Port B at 11 feet, and Port C at 51 feet) in the UCAP3 SEAMIST™ vapor sampling system. Data were collected on three separate occasions for approximately three days. The concentration levels of the detected contaminants are given in Table 3. Three generalizations can be made: the contaminant concentrations are constant with time at a particular depth, the concentrations increase with depth, and not all contaminants are present in all depths. Typical concentration profiles of three contaminants over time are shown in Figure 18.

---

<sup>1</sup> From materials contributed by G. Laguna

Table 3. Summary (average) concentration results.

| Compound                    | Port A<br>(ppm) | Port B<br>(ppm) | Port C<br>(ppm) | Run |
|-----------------------------|-----------------|-----------------|-----------------|-----|
| Pentane                     | —               | 11              | 11              | 1   |
|                             | —               | —               | 13              | 2   |
|                             | —               | —               | 18              | 3   |
| Freon 113                   | 4               | 7               | 14              | 1   |
|                             | 5               | —               | 15              | 2   |
|                             | 6               | 6               | 22              | 3   |
| 1,1,1-Trichloroethane (TCE) | 4               | 6               | 22              | 1   |
|                             | 5               | 7               | 25              | 2   |
|                             | 10              | 10              | 39              | 3   |
| Trichloroethylene           | 8               | 25              | 120             | 1   |
|                             | 10              | 22              | 115             | 2   |
|                             | 40              | 40              | 230             | 3   |
| Tetrachloroethylene (TetCe) | 3               | —               | 5               | 1   |
|                             | —               | 4               | 6               | 2   |
|                             | —               | 5               | 11              | 3   |
| 1,2-Dichlorobenzene         | —               | 4               | —               | 1   |
|                             | —               | 1               | —               | 2   |
|                             | —               | 2               | —               | 3   |

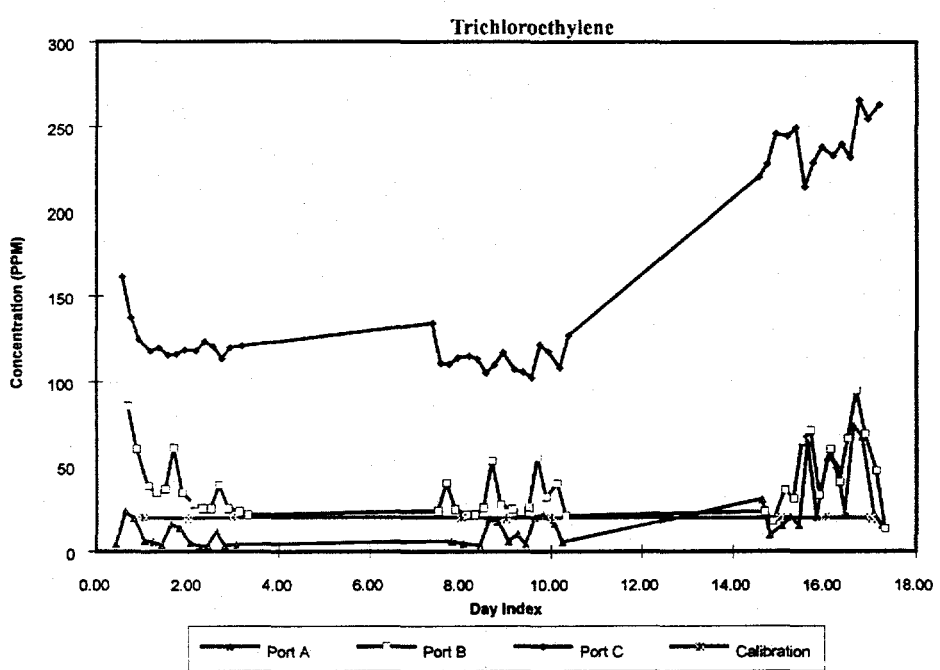
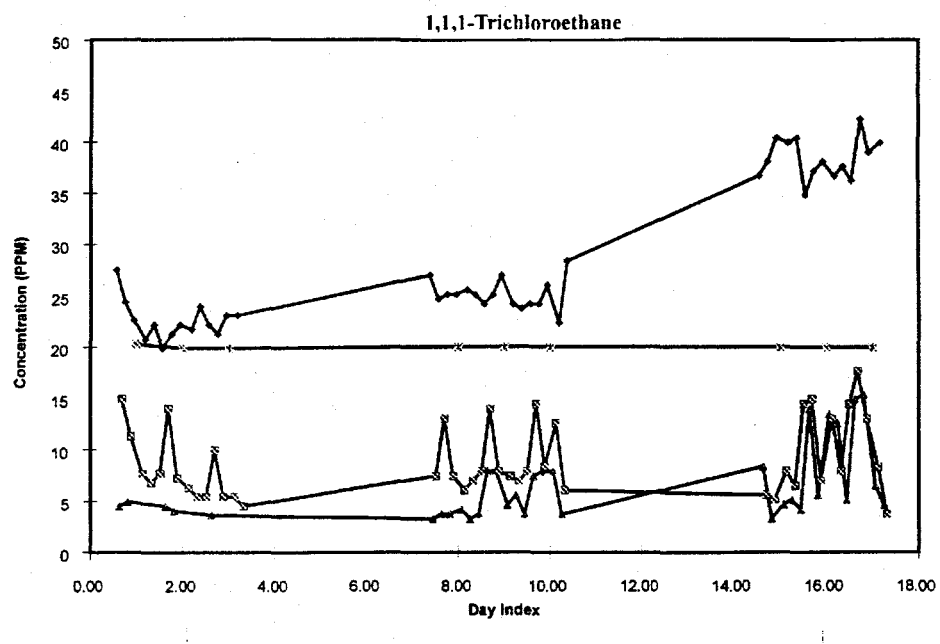


Figure 18. Contaminant histories from automated GC analysis of soil gas drawn from SEAMIST™ sampling tubing.

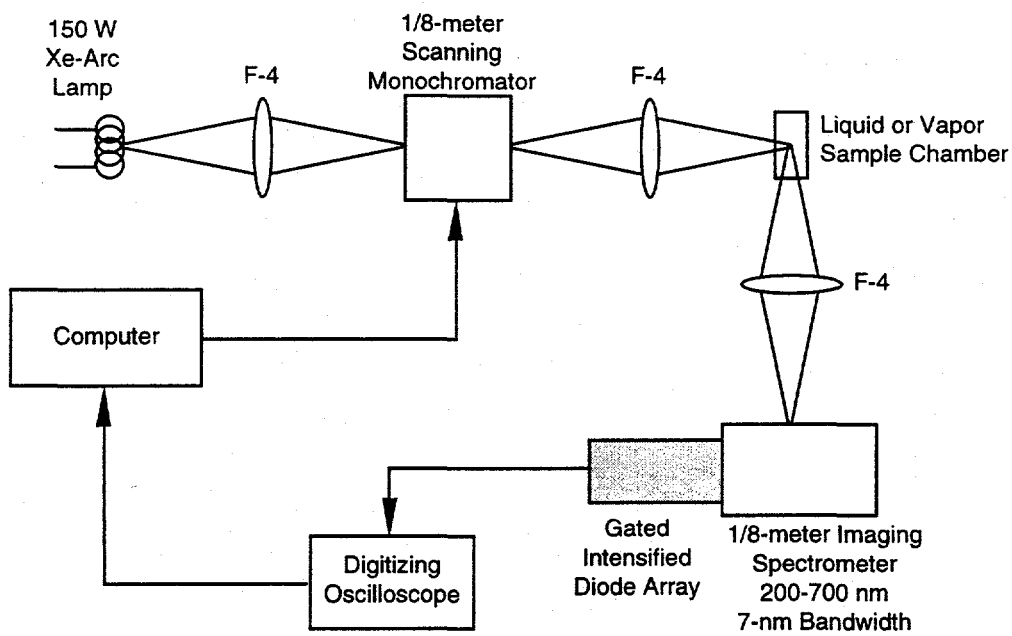
**Intentionally Left Blank**

## ULTRAVIOLET FLUOROMETER MEASUREMENTS<sup>2</sup>

An ultraviolet imaging fluorometer, developed previously at SNL to detect volatile compounds in the atmosphere, was modified for the field measurements. The fluorometer uses tunable ultraviolet light to disperse fluorescence radiation from irradiated samples. The resulting excitation spectrum is detected and displayed to show both fluorescence and adsorption signatures. A schematic diagram of the SNL ultraviolet imaging fluorometer is shown in Figure 19.

The field measurements were conducted to verify concentrations of toluene, identify potential fluorometer measurement problems, and establish measurement methodologies. Fluorometer measurements were made over three hours on borehole gases sampled at depths of 6, 51, and 81 feet in borehole UCAP3.

Fluorometer measurements were limited because solar background radiation entered the apparatus through an exhaust vent opening and increased the toluene detection limits from ~ 6 ppm to ~ 100 ppm. Therefore, good spectra from concentrations of toluene in the 10 ppm range could not be obtained. However, the test provided valuable data on the field performance of the fluorometer, and modifications to eliminate the background radiation problems were subsequently made.



TRI-6621-129-0

Figure 19. Schematic diagram of ultraviolet fluorometer.

<sup>2</sup> From material contributed by P. Hagis.

**Intentionally Left Blank**

## ASSESSMENT OF SOIL VAPOR MOVEMENT RESULTING FROM BAROMETRIC PUMPING

### Background

Advective movement of soil vapors occurs because of barometric pumping, pore size alteration resulting from saturation changes and earth tides (driven by the lunar cycles), temperature gradients, and raising or lowering of the water table. The most pronounced of these causes in the CWL setting is probably barometric pumping. The other cause for advective movement at CWL can be eliminated for a number of reasons. Earth tides have been observed to cause measurable flow in fractured rock where the flow channels are concentrated in fractures. This is not true for alluvium, the geologic setting of the CWL, where the flow is uniformly distributed throughout the porosity of the granular nature of the alluvium. Vertical movement of the water table at SNL is not likely to influence the vapor flow significantly because surface to groundwater is approximately 485 ft. Temperature gradients occur near the surface and are probably a major contributor to near-surface vapor movement, but they are not likely to strongly influence vapor movement at depths below the disposal pits.

Barometric pumping of soil gas results from the cyclic variations in the atmospheric pressure caused by daily heating and cooling cycles and occasional weather front movements (usually on 100 to 200-hour cycles). The daily atmospheric pressure cycles and the pressure response at depth, measured at the CWL are shown in Figure 20 for a one week period in June 1993. The amplitude of the daily surface variation is on the order of 5 millibars. Barometric pressure changes caused by the movement of weather fronts can result in total changes of 40 to 60 millibars at a slower rate over a longer time frame. The effect of this oscillatory boundary condition is depicted in Figure 21. In a very simplified model, assuming homogeneous soil and a rapid pressure response in the soil at depth to surface variations (i.e., a quasi-steady-state condition) a molecule of vapor in the soil will move vertically a distance proportional to the ratio of the pressure change to the absolute pressure:

$$\Delta \ell = \frac{\Delta p}{P_{atm}} \times L \quad (2)$$

where:

$\Delta p$  = cyclic pressure variation  
 $P_{atm}$  = nominal absolute (barometric) pressure  
 $L$  = distance to an impermeable boundary such as the water table

A fairly rapid response at depth (to 95 feet bgs) to surface pressure fluctuations has been observed, as shown in the plot of Figure 20. The pressure response at depth is virtually immediate on this time scale, indicating a quasi-steady-state flow condition.

Because the depth to groundwater at the CWL is approximately 485 feet, a daily 5 mbar barometric pressure variations would result in total vertical displacement,  $\Delta \ell$ , of a gas molecule at the 20-foot depth of 2.8 ft.

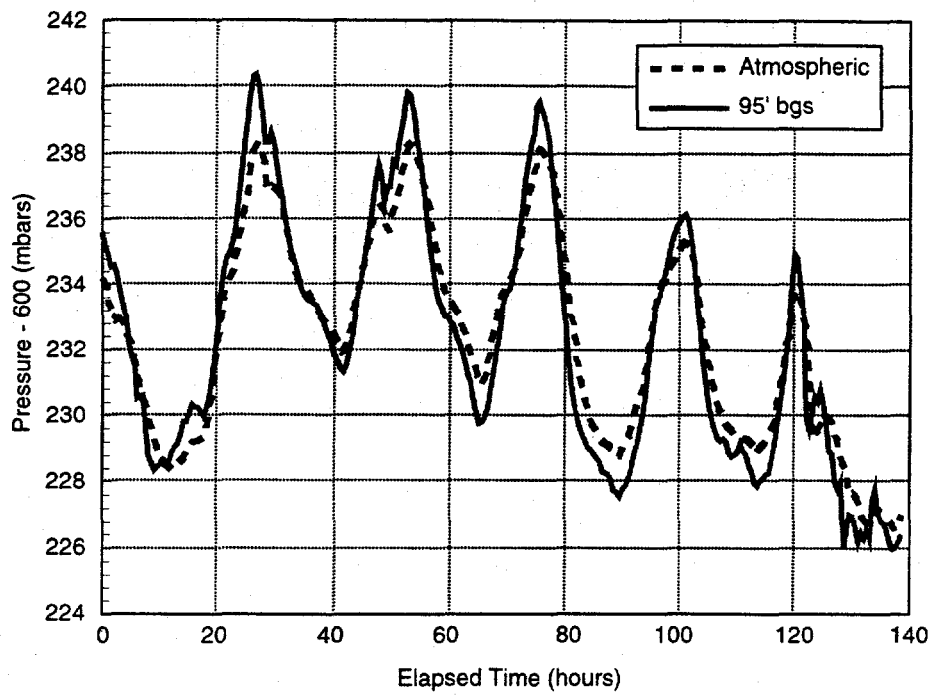


Figure 20. Comparison of surface barometric pressure with pressure at depth for UCAP3.

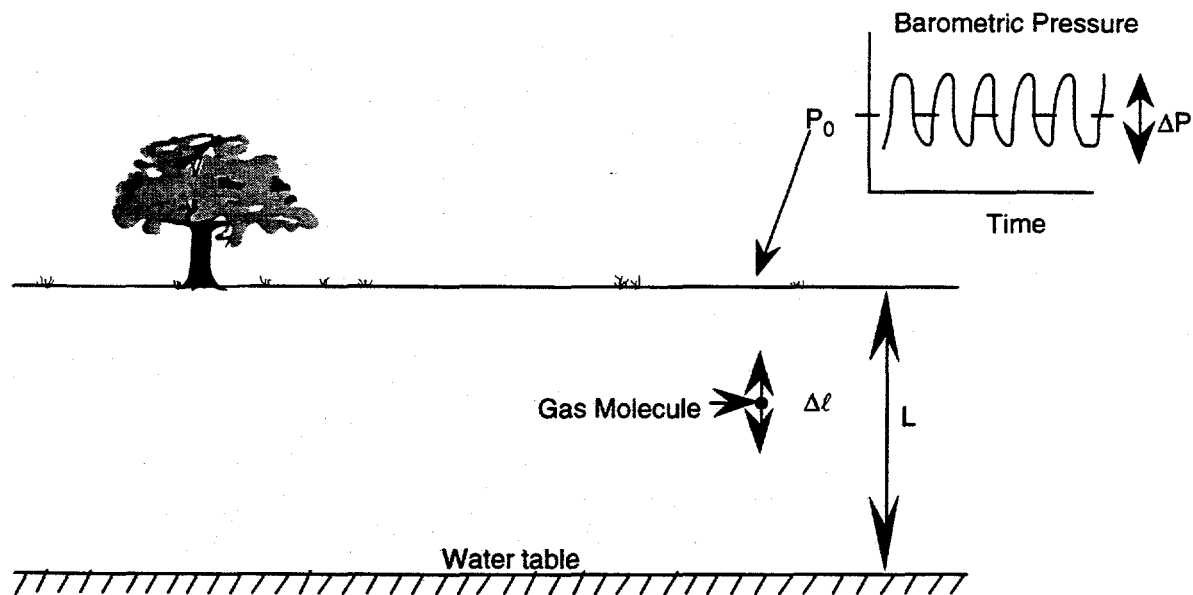


Figure 21. Simplified model of the effect of barometric pressure on soil vapor movement at depth.

$$\Delta\ell = \frac{5 \text{ mbar}}{830 \text{ mbar}} \times (485' - 20') = 2.8 \text{ ft} \quad (3)$$

where 830 mbar is the average barometric pressure at the site.

For the larger pressure variations (60 mbar) associated with weather fronts, the maximum displacement would be 33.6 ft:

$$\Delta\ell = \frac{60}{830} \times (485 - 20) = 33.6 \text{ ft.} \quad (4)$$

Two features of the real soil environment cause departures from this simple model, one potentially increasing and the other decreasing the total displacement.

If the soil is homogeneous and isotropic, the net vertical movement of the vapor molecule at depth will be zero over time, because the barometric pressure always returns to a mean value. However, laboratory tests have shown that the vertical movement can be amplified and result in a net displacement if soil heterogeneities are present (Peterson, et al., 1987). This ratcheting occurs because as soil gas flows upward in its regular cycle, it travels farther in some areas than others due to heterogeneities in the soil properties. Contaminants will diffuse laterally from these leading fronts due to concentration gradients but do not necessarily diffuse back into the plume on the reverse cycle. The effect is greatest in the case of vertical fractures and can result in a hundred-fold increase in the transport rate compared to the diffusion rate. An extreme case of ratcheting occurs when the contaminant is sufficiently close to the surface resulting in its release into the air during its maximum vertical displacement.

The second effect will decrease the displacement. The oscillatory flow of Equation 2 is an absolute maximum case, assuming a steady-state condition. The resistance to gas flow caused by the soil's permeability dampens the soil gas pressure response, preventing the attainment of a true steady-state condition. The soil gas at depth never has quite enough time to fully equilibrate with the surface pressure because the surface pressure is constantly changing. The downhole response slightly lags the surface pressure, even though in Figure 20 the surface and 95-foot depth pressure histories look in phase.

### Vapor Movement Test

The large scale vapor movement test was conducted at the CWL. The disposal pit involved in this experiment is the UCAP, in which liquid chromic acid was disposed. The instrumented SEAMIST™ membranes were installed in all three of the UCAP boreholes to support the Thermally Enhanced Vapor Extraction System (TEVES) experiments and the vapor movement test. Several Geoprobe points were also installed in support of TEVES. The relationships between the UCAP and Geoprobe installations are depicted in the two dimensional and three-dimensional representations shown in Figures 22 and 23.

Permeability measurements had been conducted previously in the two TEVES wells and the three UCAP wells. Two different systems were used for the measurements. A SEAMIST™ membrane system was used to measure the permeability distribution in the TEVES boreholes. A dual packer system was used for measurements in the UCAP wells. Measurement techniques and models are discussed in the report by Phelan (1993).

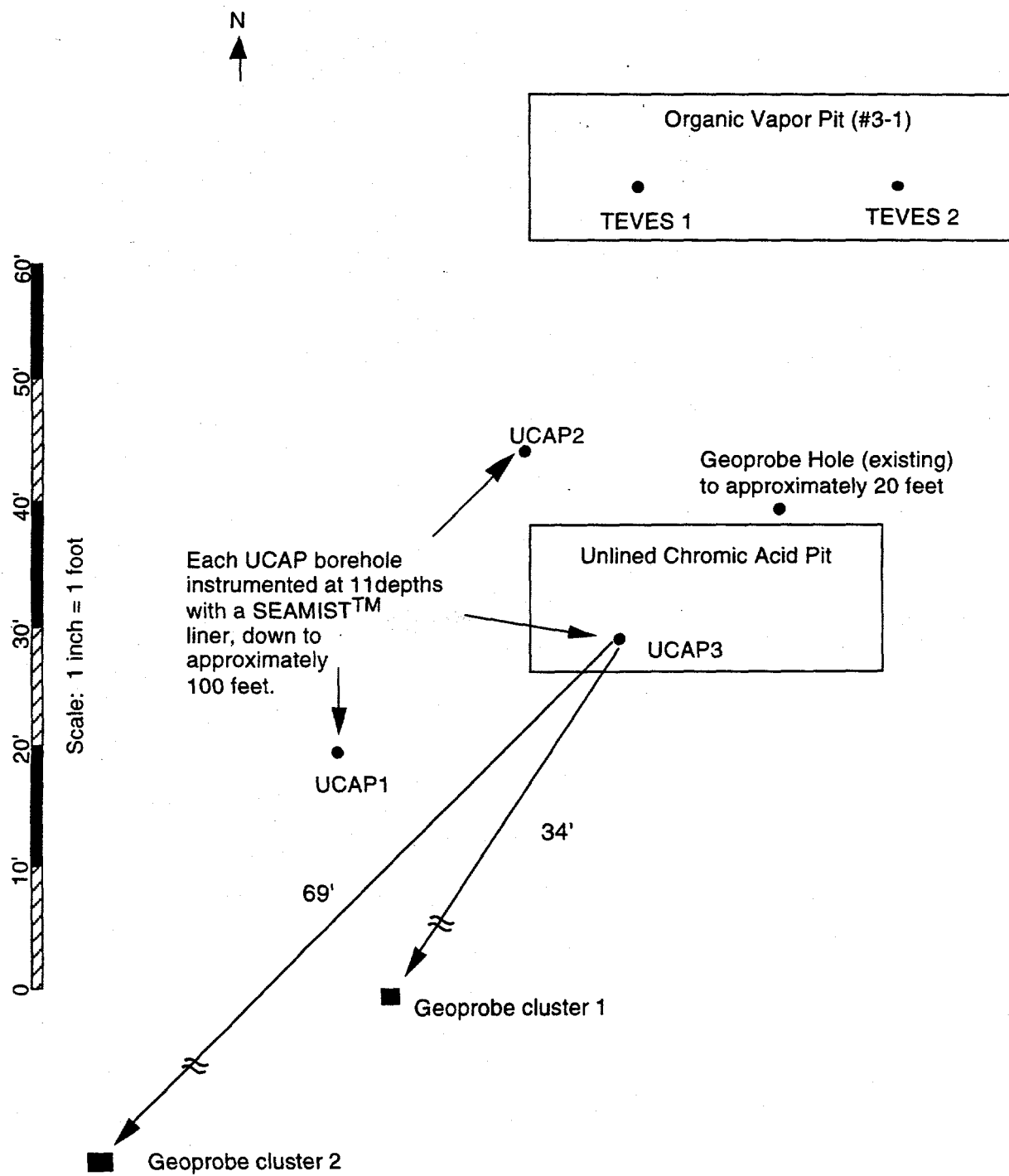


Figure 22. Plan view of the UCAP, TEVES, and GeoProbe installations.

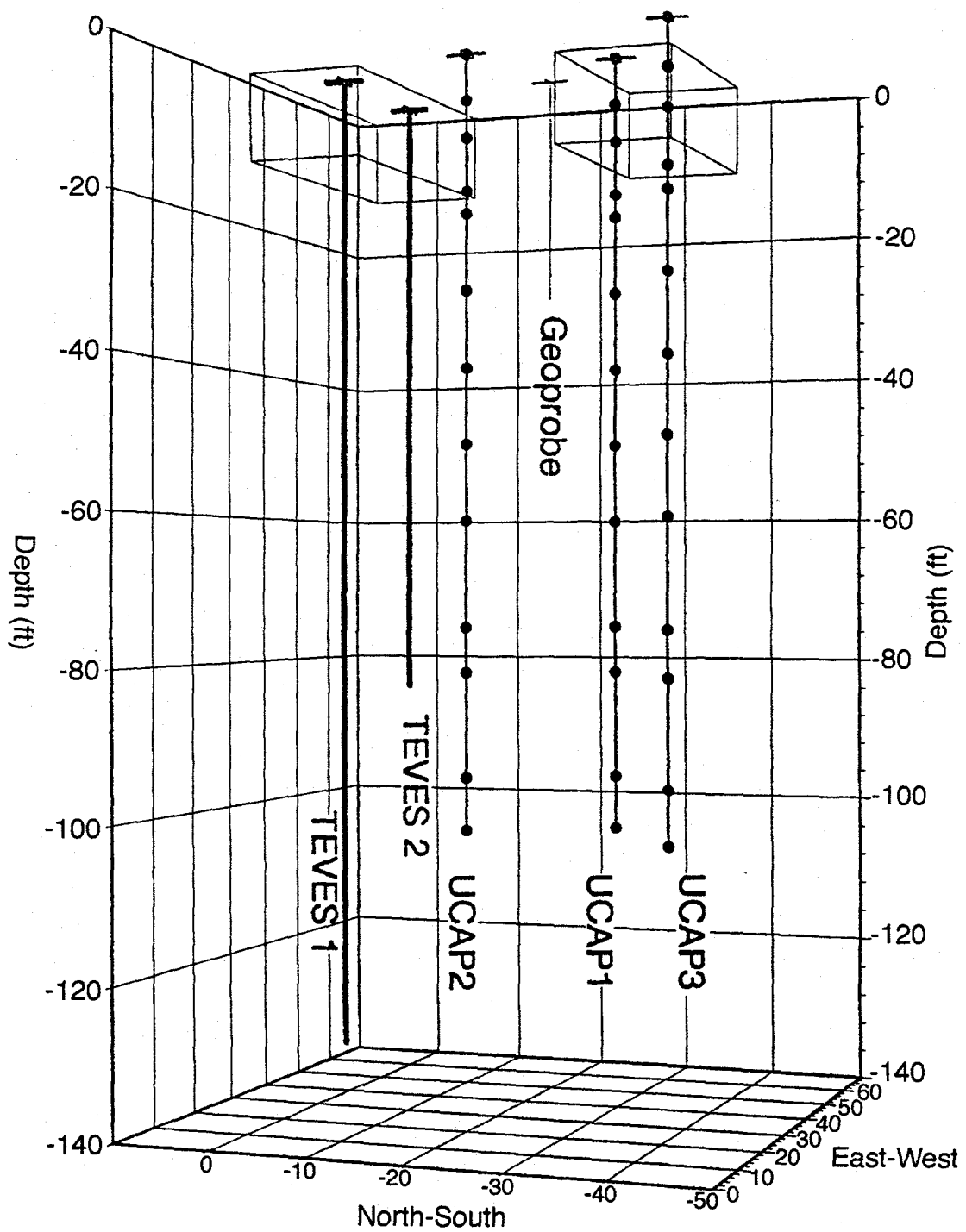


Figure 23. Three-dimensional layout of the UCAP boreholes.

The TEVES permeability measurement results are shown in Figure 24. These results that are included to indicate the range of permeabilities measured of the area were not used in the subsequent analysis. The UCAP results are given in Figure 25. Permeabilities vary widely, from two up to several hundred darcies, but most of the measured values are below 20 darcies. In Figure 26 we have also shown the averages used over selected intervals for the vapor movement calculations. The data were collected using the Campbell Scientific CR-7 Datalogger System (p. 9)

The surface and in-situ gas pressures were recorded every 30 minutes for the 140-hour test duration analyzed. The scanning system completed its sweep of the pressure sensing lines in 4 minutes. Each sensing location required 5 seconds to equilibrate and measure. A ribbon plot of a typical multipoint pressure history is depicted in Figure 26. The gas at depth responds very quickly to surface perturbations because very little gradient is measured (typically 1.0 to 1.5 mbar over the full 95-foot depth).

The pressure data were used to assess the quality of the borehole seal, which must be adequate for the vapor movement calculations to be valid. The SEAMIST™ membrane forms a low pressure seal of the borehole because it operates in the neighborhood of 1 psi overpressure. Pressure records from specific elevations on the SEAMIST™ membranes are compared with corresponding elevations in Geoprobe installations. In Figure 27, measurements at the 20-foot Geoprobe ports and the 21-foot SEAMIST™ ports are compared. Atmospheric pressure and the pressure at 95 feet are also plotted for comparison. Within normal data variability, the SEAMIST™ port system result in virtually identical pressure responses as corresponding Geoprobe installations. Consequently, for this application in this medium, the membrane seal is adequate.

### Net Soil Gas Displacement

The movement of soil gas can be estimated from the pressure gradient in the soil and the soil permeability. The straddle packer measurements conducted in the UCAP boreholes (Figure 25) are used to estimate the permeability distribution in the soil. The permeability is combined with the pressure gradients measured with the SEAMIST™ systems to estimate soil gas velocity histories at specific depths in the soil.

For very small pressure fluctuations caused by small barometric changes on the order of 5 millibars, air flow in soils can be considered incompressible. A simple Darcy flow model predicts steady state porous flow under these conditions:

$$Q = \left( \frac{kA}{\mu} \right) \left( \frac{\Delta p}{L} \right) \quad (5)$$

where:

$Q$  = volumetric gas flow through soil

$k$  = permeability of soil

$A$  = cross sectional area

$\frac{\Delta p}{L}$  = pressure gradient in soil ( $L$  = measurement point spacing)

$\mu$  = soil gas viscosity

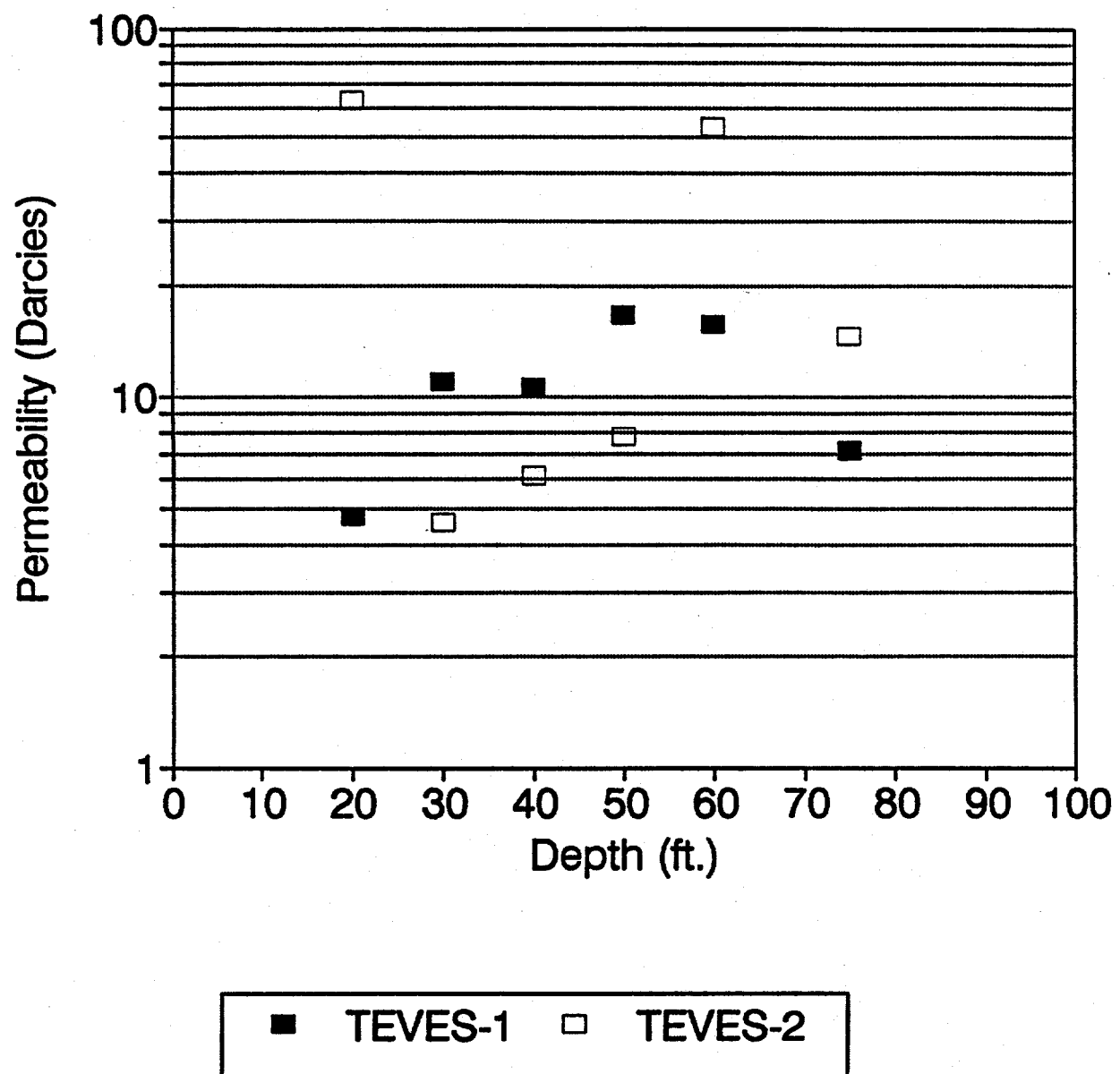


Figure 24. Permeability measurement results for the TEVES boreholes (Phelan, 1993).

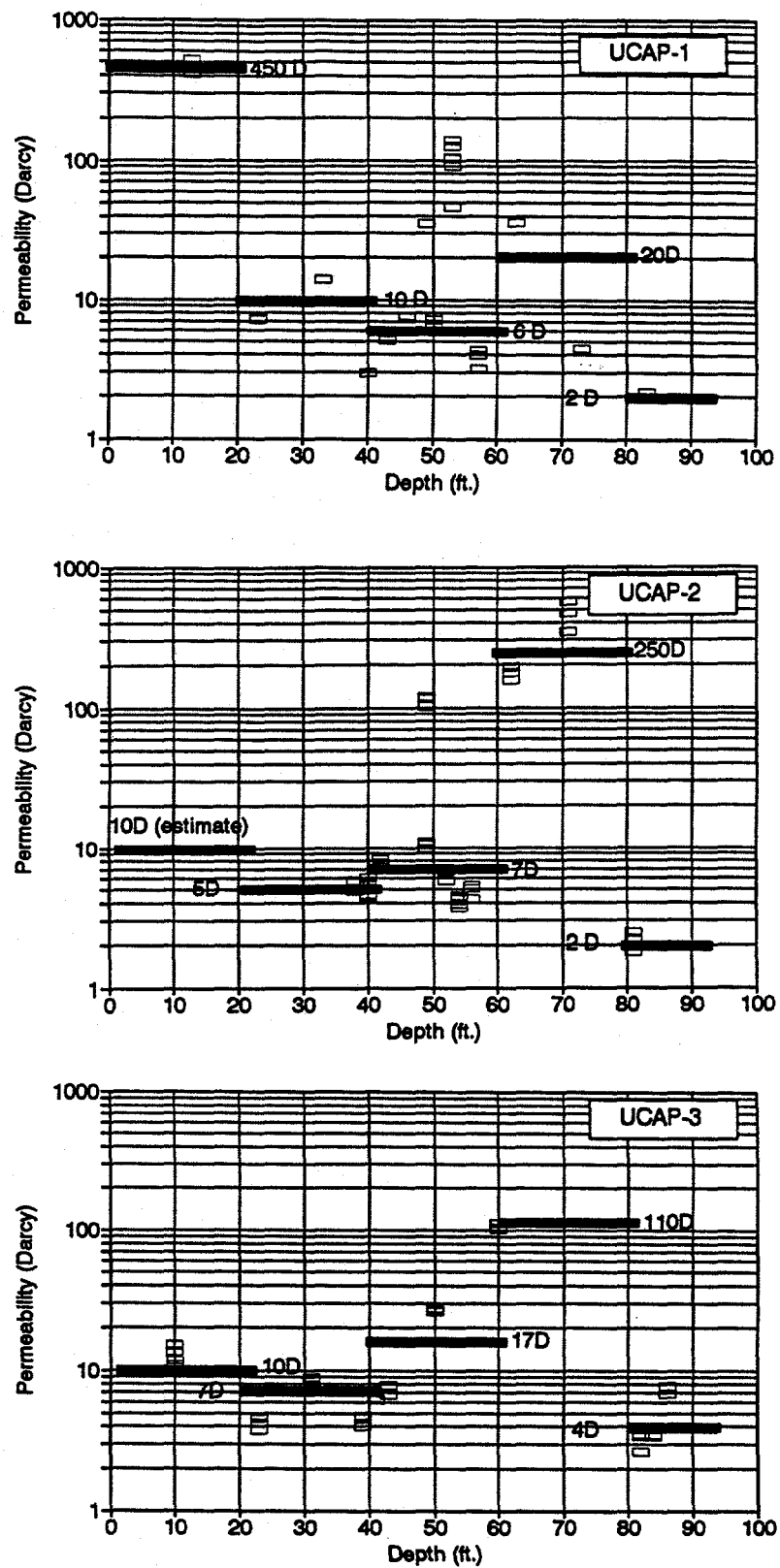


Figure 25. Permeability measurement results for the UCAP boreholes. The solid horizontal bars represent the average values for the indicated depth interval.

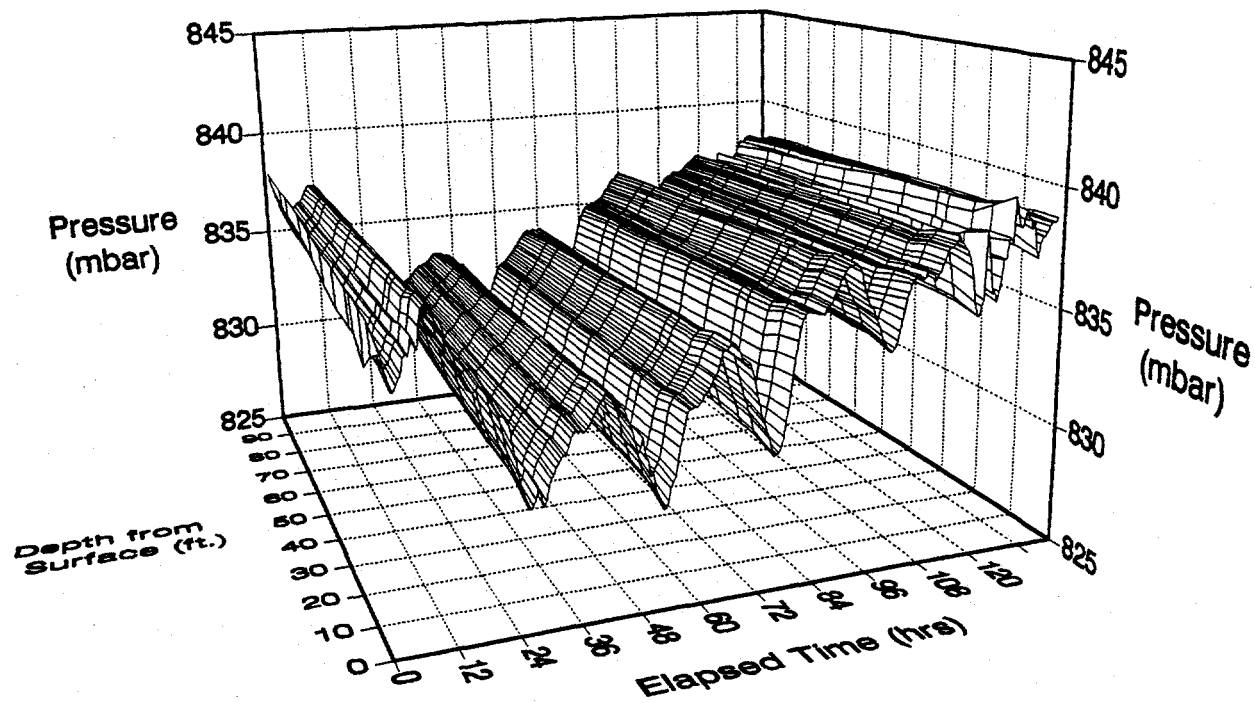


Figure 26. Pressure history versus depth for UCAP3.

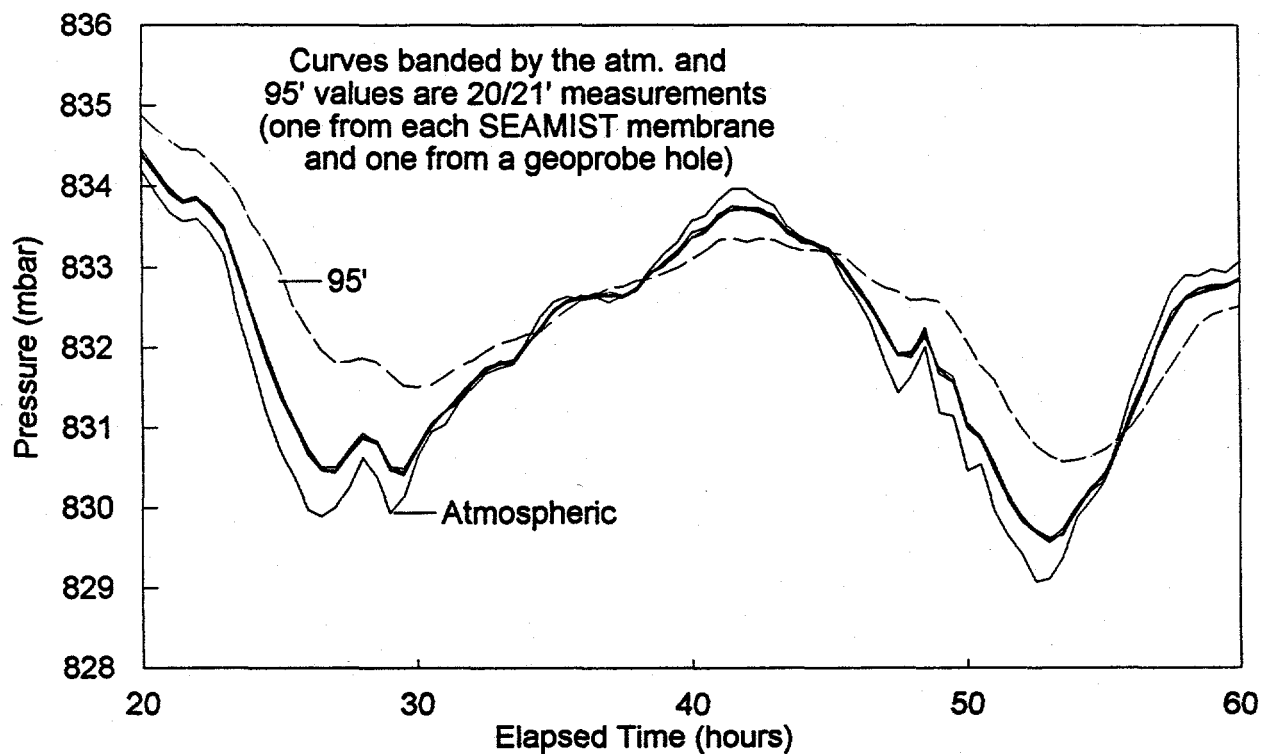


Figure 27. Comparison of pressure responses from SEAMIST™ pressure ports and Geoprobe ports at depths with atmospheric pressure and soil gas pressure at 95 feet.

The gas permeability over the interval is taken from Figure 25, where the measured values have been averaged. Calculations were done over roughly 20-foot intervals because the pressure differentials were too small at finer spacings for adequate precision in the calculation.

The net velocity of gas in the soil is given by:

$$V = \frac{Q}{A \cdot \phi} \quad (6)$$

where:

$\phi$  = porosity of the soil accessible to soil gas.

To determine displacement of the soil gas, the velocity is integrated over time.

A 140 hour data set was analyzed. A typical sequence of calculations is shown in Figure 28, showing the progression from the recorded pressures (uncorrected), to pressure gradient, velocity, and integrated displacement. The resulting velocity and displacement histories for all points measured are shown for a 140-hour period in Figures 29, 30 and 31 for UCAP1, 2, and 3 respectively. The recording period centered about a barometric low, which is apparent in Figure 27 if the daily fluctuations are averaged. Consequently, the plots in Figures 29 through 31 show a rise and then fall in the vapor displacement. The daily cycles appear on the displacement histories but are less than 20 percent of the displacement because of the slower low pressure front. The displacements scale with the permeability, so the high estimated displacement at 10.5 feet in UCAP1 is attributed to a very high permeability of 450 Darcies measured at that location (Figure 25). As much as 4 meters of vertical displacement are estimated at this location, whereas at other depths in the borehole the displacement is less than 15 cm. In UCAP2, at 71 feet, the displacement is also relatively high because of the corresponding high permeability at that location (250 darcies).

### Inferring Vertical Permeability with Transient Pressure Data

The measured response of the soil gas at depth to the periodic surface pressure oscillations provides an opportunity to infer the vertical permeability of the soil. The following model development capitalizes on the attenuation of the pressure oscillations at depth to estimate a bulk diffusivity. This technique has been used to estimate vertical contaminant flow on very large scales (Nilson, et al., 1981).

The diffusivity of a homogeneous medium is,  $\alpha$ , is given by:

$$\alpha = \frac{kP_0}{\mu\phi} \quad (7)$$

where:

$k$  = permeability,

$P_0$  = static pressure,

$\mu$  = gas viscosity, and

$\phi$  = accessible gas-filled porosity,

and the pressure field  $[p(x, t)]$  responds to barometric pressure changes in accordance with

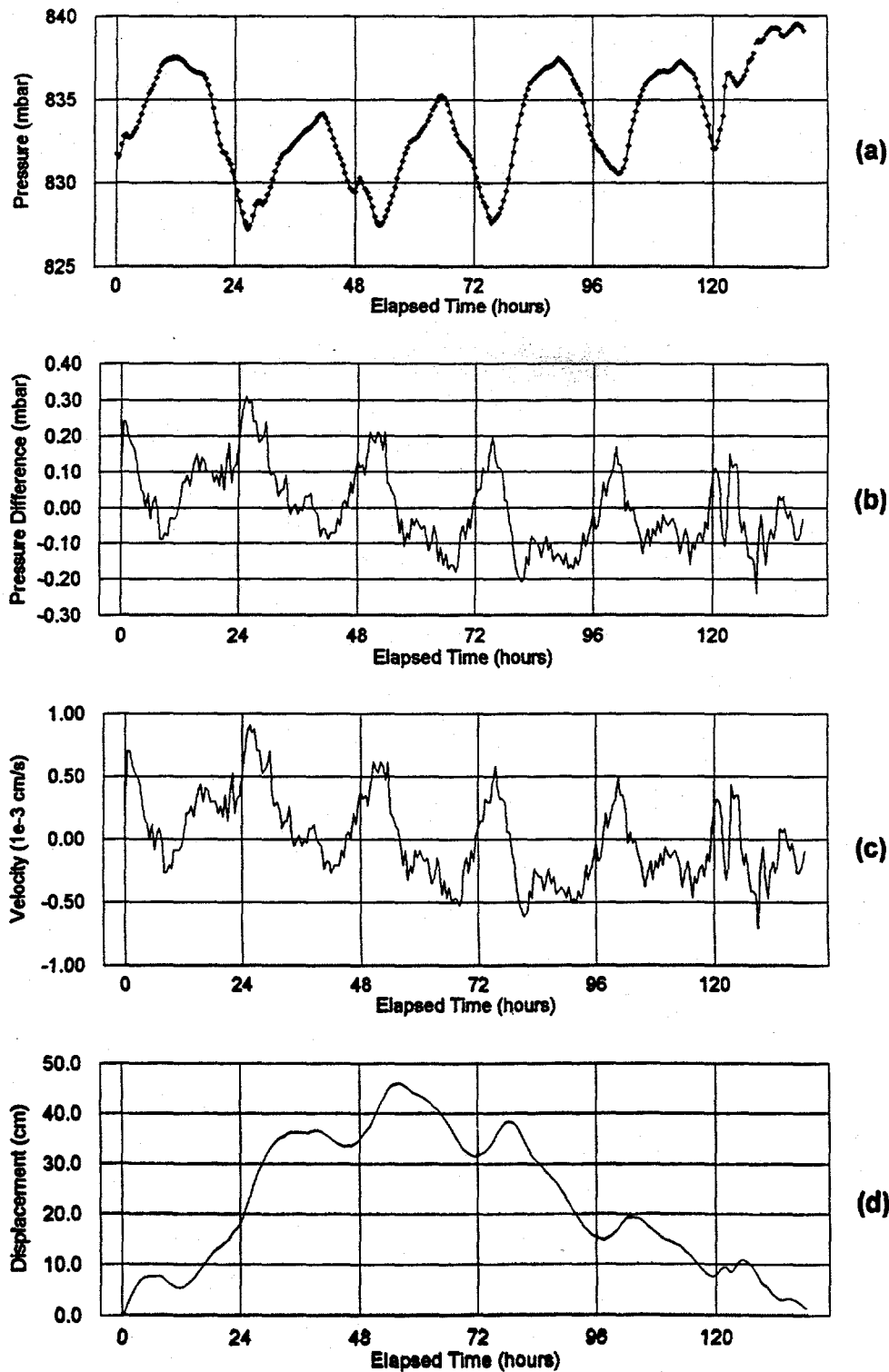
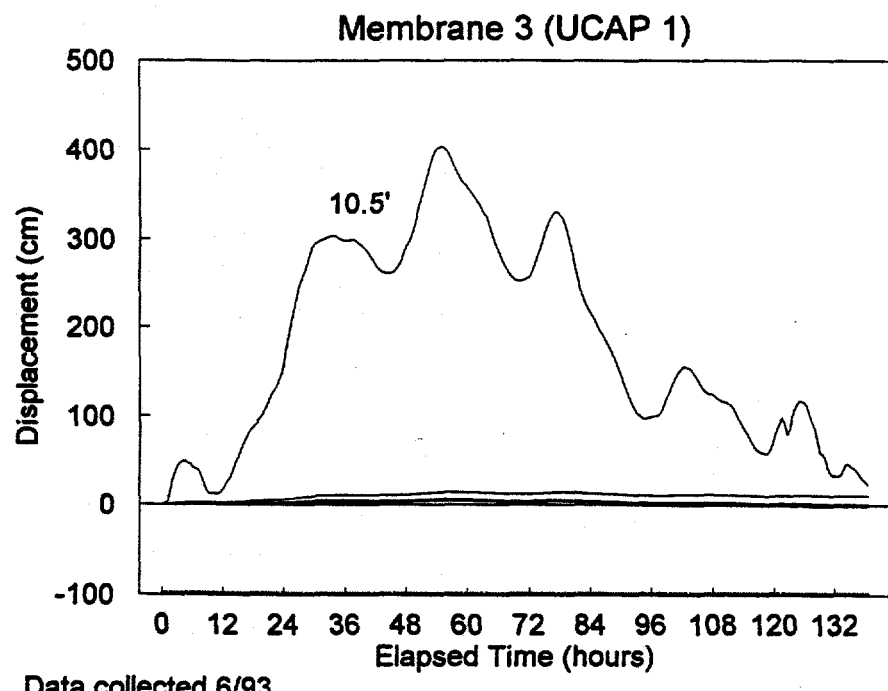
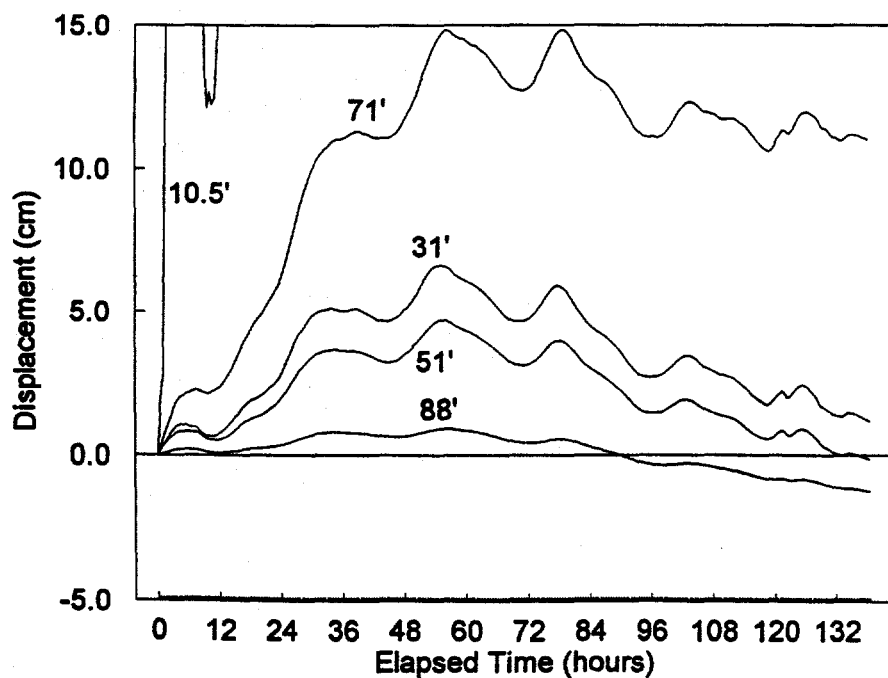


Figure 28. Calculational sequence to determine vapor displacement: a) recorded pressure data, b) pressure difference, c) gas velocity, and d) displacement.

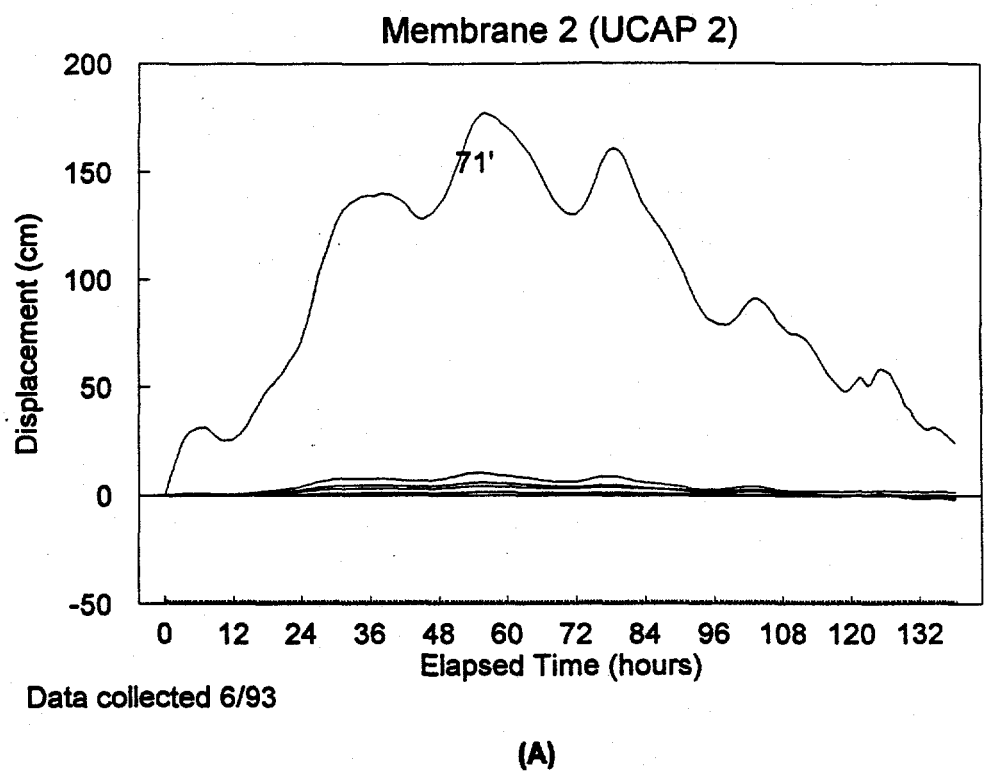


**(A)**

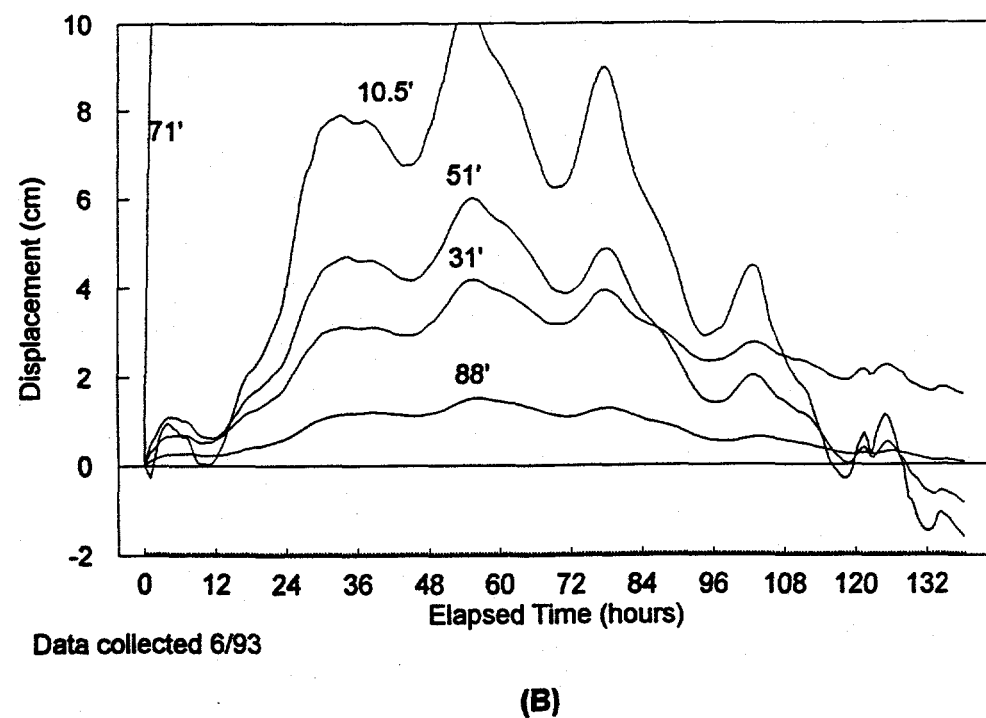


**(B)**

Figure 29. Displacement calculations for UCAP1.

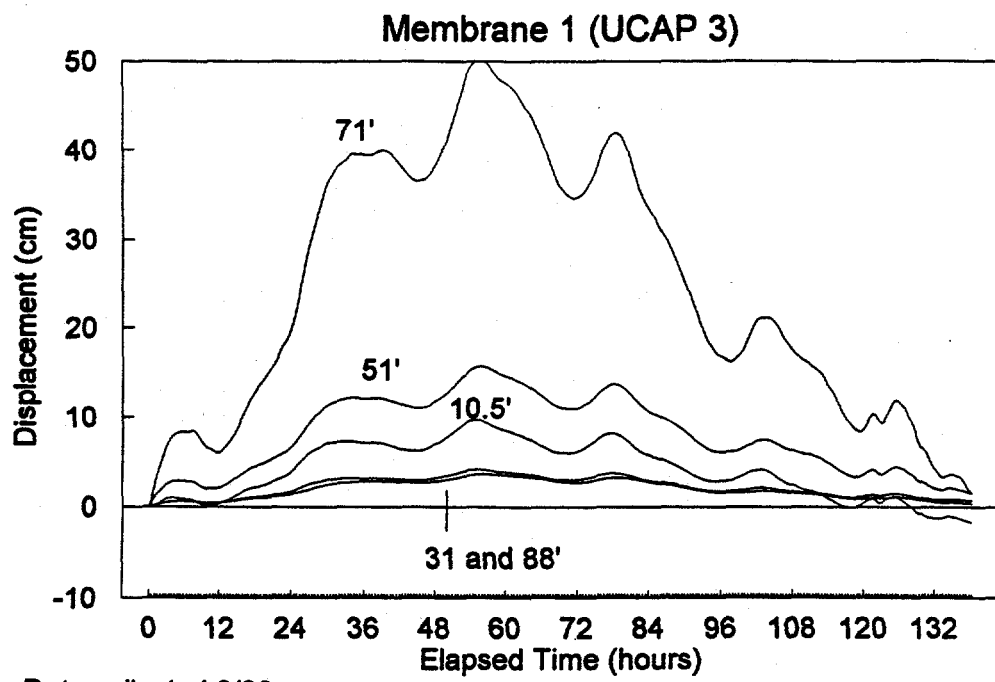


**(A)**



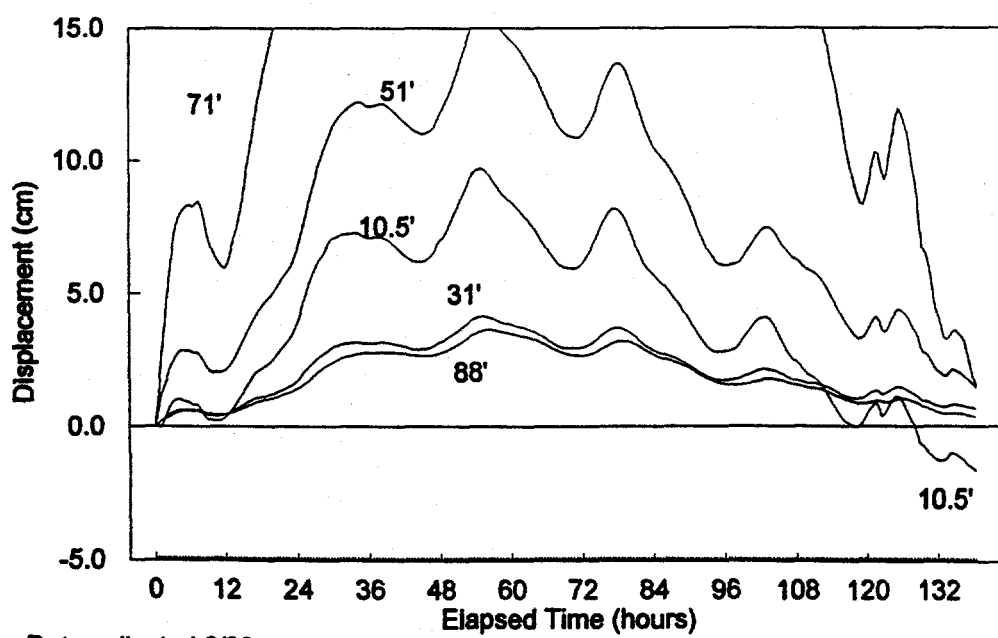
**(B)**

Figure 30. Displacement calculations for UCAP2.



Data collected 6/93

**(A)**



Data collected 6/93

**(B)**

Figure 31. Displacement calculations for UCAP3.

$$\frac{\partial^2 p(x, t)}{\partial x^2} = \frac{1}{\alpha} \frac{\partial p}{\partial t}, \quad (8)$$

where  $x$  is the depth and  $t$  is time. For a no-flow boundary at  $x = L$  and the periodic surface pressure

$$p(0, t) = p_0 + \Delta p e^{i\omega t}, \quad (9)$$

the resulting pressure field is

$$p(x, t) = p_0 + \Delta p \frac{\cosh[\lambda\sqrt{i}(i - x/L)]}{\cosh \lambda\sqrt{i}} e^{i\omega t} \quad (10)$$

where  $\lambda = L\sqrt{\omega/\alpha}$ . That is, the pressure at depth is also periodic with frequency  $\omega$ , but has an amplitude decrease and a phase shift.

Replacing  $\sqrt{i}$  with its equivalent,  $(1+i)/\sqrt{2}$ , the amplitude ratio  $R(x)$  is

$$R(x) = \frac{\left| \cosh \frac{\lambda}{\sqrt{2}} (1 - \frac{x}{L})(1+i) \right|}{\left| \cosh \frac{\lambda}{\sqrt{2}} (1+i) \right|} \quad (11)$$

using the formula

$$|\cosh y (1+i)|^2 = \cosh^2 y \cos^2 y + \sinh^2 y \sin^2 y = \frac{1}{2} ((2 + \cosh 2y + \cos 2y))$$

$$R^2(x) = \frac{2 + \cosh [\sqrt{2} \lambda (1 - x/L)] + \cos [\sqrt{2} \lambda (1 - x/L)]}{2 + \cosh \sqrt{2} \lambda + \cos \sqrt{2} \lambda} \quad (12)$$

For a relevant range of conditions, this calculational sequence is expressed in Figure 31. Pressures for the surface pressure and the 95-foot-deep soil gas pressure are shown in Figure 32(a). A Fast Fourier Transform (FFT) is applied to each of these data records to determine relative amplitudes versus frequency. These are plotted in Figures 32(b) and (c). The FFT allows us to systematically determine relative amplitudes when the recorded data include a mix of frequency components such as the well-defined 24-hour cycle and the slower weather front cycle. The ratio of these amplitudes is then calculated and evaluated specifically at the frequency of interest (Figure 32(d)). Using Equation 12 with the amplitude ratio and  $x/L$  as inputs, the Fourier modulus  $M = (aT/L^2)$  is determined. The relationship is plotted in Figure 33. The diffusivity is calculated as:

$$\alpha = \frac{L^2}{T} \cdot M \quad (13)$$

and the permeability is:

$$k = \frac{\mu \phi}{\alpha P_0} \quad (14)$$

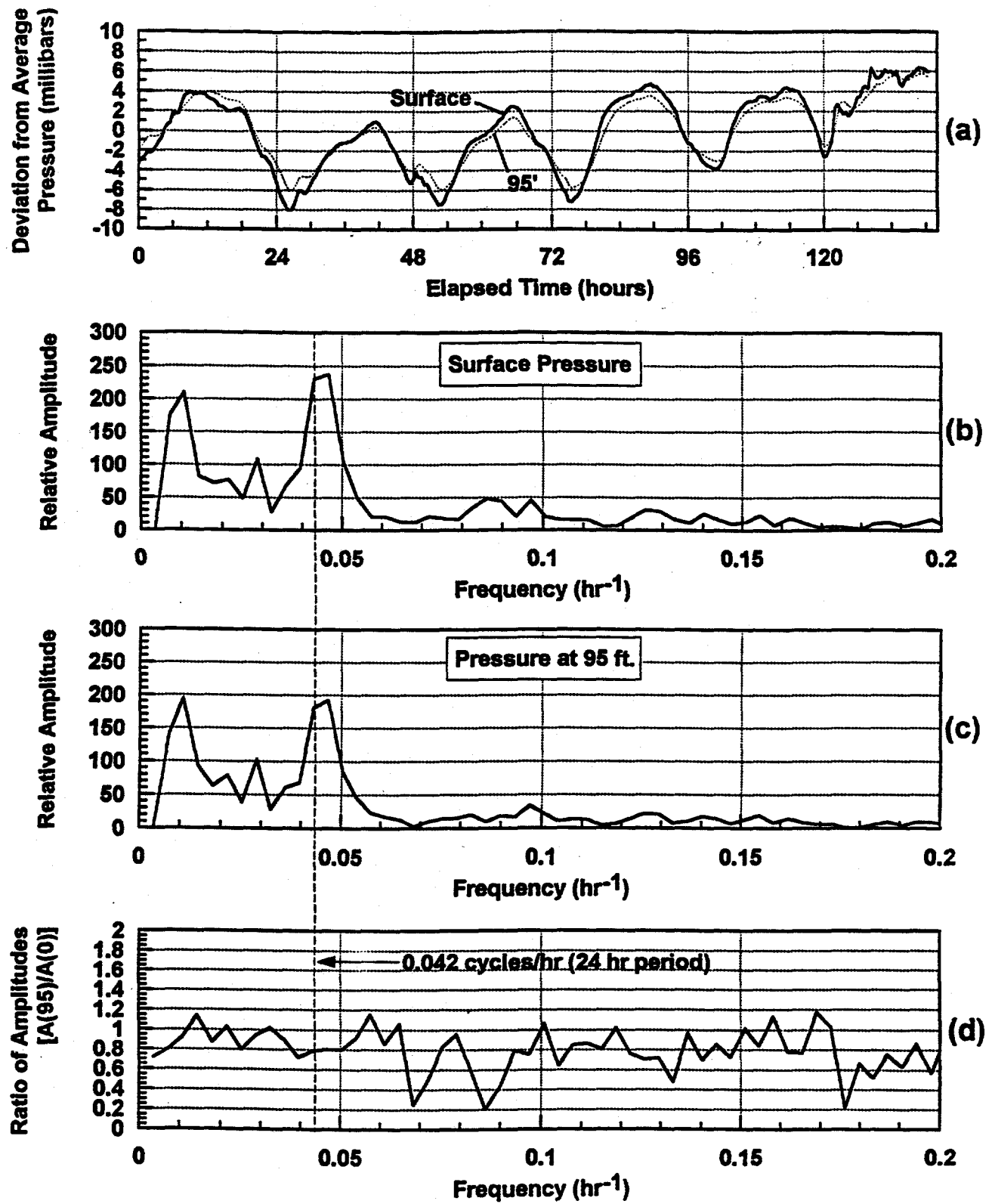


Figure 32. Time series analysis sequence to determine amplitude ratio between the surface pressure and the soil gas pressure at 95-foot depth.

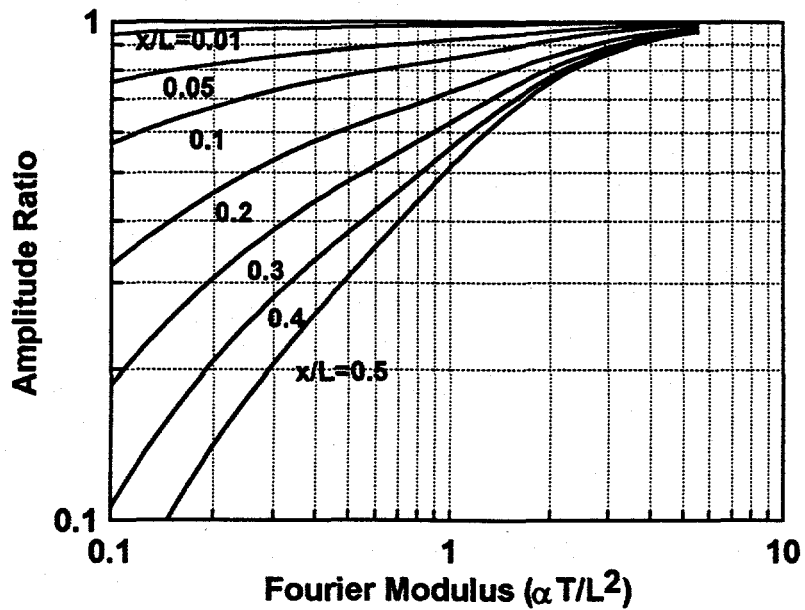


Figure 33. Relationship between Fourier modulus and amplitude ratio.

This technique was applied to all of the available pressure measuring points from the June 15 record. Porosities were determined from the UCAP samples (Ref. 3) and are listed in Table 4. All of the resultant permeabilities are plotted in Figure 34. Several features of this graph are noteworthy. First is that the permeability approaches a constant value of 10 darcies as the measurement depth increases. The model assumes a homogeneous medium above and below the measurement point. The values plotted in Figure 34 are the average vertical permeability of the total medium deduced using a pressure history at that particular depth. Note: this is not a plot of permeability versus depth. The data in the top 30 feet of the borehole are probably more influenced by the variability observed in that region (from permeability measurements) than deeper measurements. At depth, there is more distance over which to average and attenuate the response. This could also be an artifact of the experiment (such as less measurement precision at the shallow depth), and further analysis is required to explain this result. The deeper results show an encouraging consistency. The 10 darcy number for the lower 70 feet of the borehole is probably a good average vertical permeability of the medium. This value is in the range of both the TEVES and UCAP in-situ permeability measurements. A second feature of this plot is that the three measurement points corrupted by rodent-damaged sensing tubes (partially or completely open to atmospheric air) are clearly identified in the graph.

Table 4. Calculated porosity of split spoon samples from the UCAP boreholes.

| Sample Depth (ft)  | UCAP1                   |                  | UCAP2                   |                  | UCAP3                   |                  |
|--------------------|-------------------------|------------------|-------------------------|------------------|-------------------------|------------------|
|                    | Volumetric Moisture (%) | Dry Porosity (%) | Volumetric Moisture (%) | Dry Porosity (%) | Volumetric Moisture (%) | Dry Porosity (%) |
| 10                 | 7.39                    | 26.91            | 12.67                   | 33.31            | 20.23                   | 43.01            |
| 20                 | 3.76                    | 38.32            | 4.26                    | 34.30            | 9.94                    | 28.18            |
| 30                 | 8.96                    | 31.53            | 6.58                    | 29.80            | 4.12                    | 28.27            |
| 40                 | 10.68                   | 33.38            | 11.66                   | 33.39            | 11.50                   | 33.39            |
| 50                 | 5.42                    | 24.39            | 5.06                    | 31.10            | 3.99                    | 26.30            |
| 60                 | 12.22                   | 37.85            | 7.97                    | 27.31            | 14.48                   | 32.31            |
| 70                 | 13.37                   | 40.80            | 4.53                    | 25.34            | 3.58                    | 29.09            |
| 80                 | 13.35                   | 35.59            | 16.06                   | 33.09            | 5.33                    | 25.61            |
| 90                 | 4.21                    | 27.58            | 2.82                    | 26.49            | 4.01                    | 31.57            |
| 100                | 7.00                    | 42.65            | 7.02                    | 30.20            | 10.30                   | 35.99            |
| 110                | 5.65                    | 41.43            | 2.17                    | 24.29            | 4.31                    | 39.93            |
| 115                |                         |                  |                         |                  | 5.70                    | 51.37            |
| 120                | 7.42                    | 41.38            | 4.86                    | 29.46            | 6.74                    | 35.09            |
| Average            | 8.29                    | 35.15            | 7.14                    | 29.84            | 8.02                    | 33.85            |
| Standard Dev.      | 3.42                    | 6.33             | 4.26                    | 3.38             | 5.06                    | 7.37             |
| Available Porosity |                         | 32.24            |                         | 27.71            |                         | 31.14            |

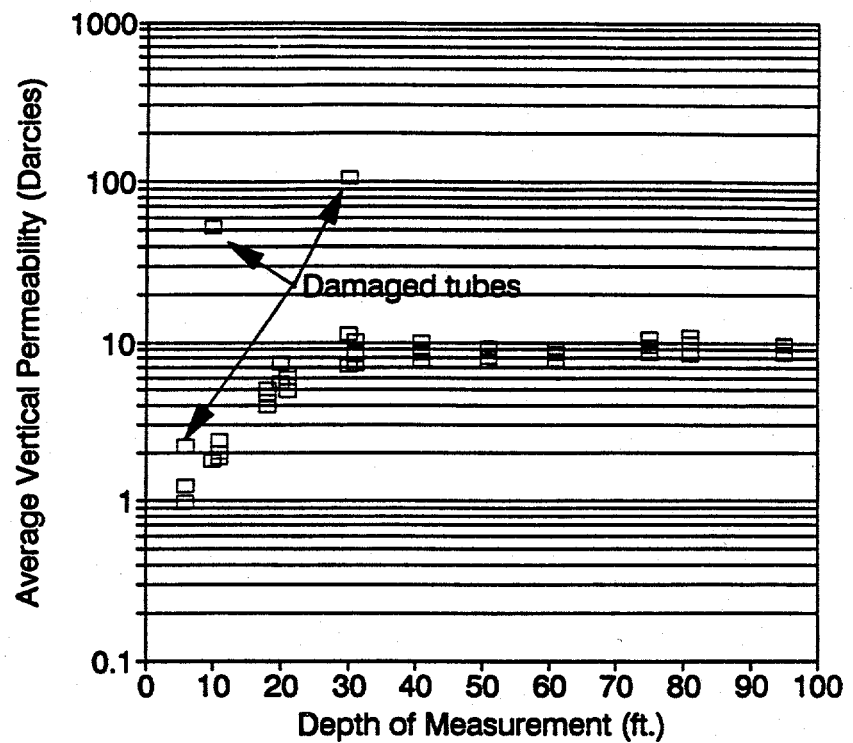
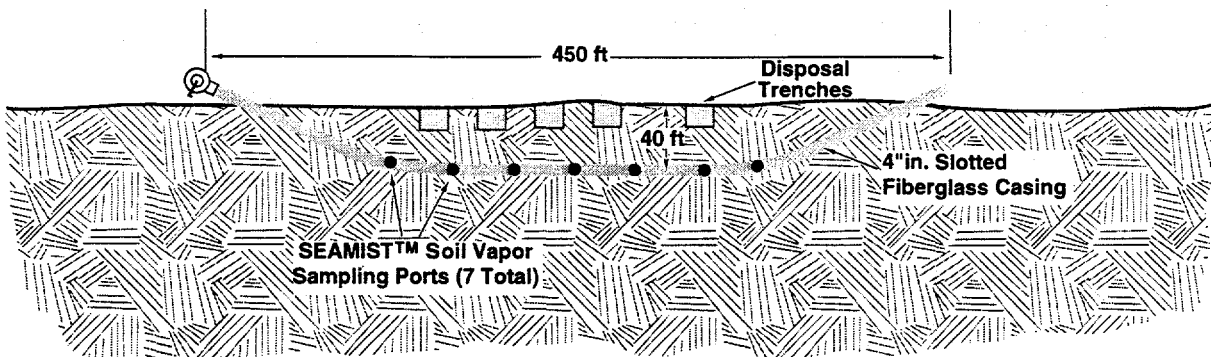


Figure 34. Resulting estimated permeabilities derived from the time series analysis (UCAP and Geoprobe measurement points). Note that this is not a plot of permeability versus depth, but a plot of overall average medium permeability derived from a measurement at the indicated depth.

**Intentionally Left Blank**

## OTHER SUPPORT ACTIVITIES

SEAMIST™ systems were also provided to support other characterization programs. A 160-foot-long, 4-inch-diameter system was fabricated with seven vapor sampling ports for use in boreholes drilled beneath the CWL "60's pits" (Figure 34). A similar system was fabricated and installed in a directionally drilled hole beneath the Kirtland Air Force Base RB-11 landfill (Figure 35). The latter installation was the most ambitious SEAMIST™ installation to date, being 400 feet long. Both these systems were installed, used, and removed.



TRI-6621-130-0

Figure 35. Schematic representation of the SEAMIST™ system installed beneath the KAFB RB-11 landfill.

**Intentionally Left Blank**

## SUMMARY AND RECOMMENDATIONS

This program tested integrated SEAMIST™/sensor systems, evaluated novel portable gas analysis systems, assessed soil vapor movement caused by barometric pressure variations, and supported slant and directionally drilled borehole measurements.

All the sensors tested were easily deployed with SEAMIST™ and automatically recorded with the Campbell Scientific CR7 data acquisition package. Once deployed, all the sensors functioned as designed, with no adverse effects caused by SEAMIST™'s unique emplacement mechanism. While monitoring/characterization of the CWL was not a primary goal of this task, data collected with the sensors was analyzed to determine the potential of the sensor to be used effectively as a monitoring/characterization device. Six physical process sensors and four chemical sensors were tested at the CWL.

Of the six physical process sensors, two measured in-situ soil gas pressure, one measured downhole temperature, and the remaining three measured hydrologic matric potential. Both methods tested for measuring in-situ soil gas pressure recorded similar pressure histories with depth, showing daily pressure variations of 5 to 8 mbar. Using a high precision pressure transducer at the surface to measure in-situ pressures transmitted through tubes that extend to the desired sampling elevation had positive features of: (1) measuring multiple sampling elevations with a single transducer; (2) using the same instrumentation with multiple SEAMIST™ systems; and (3) accessing easily the instrumentation for calibration or repair. The main drawback with the pressure transducer tested was its sensitivity to temperature fluctuations. This problem can be minimized by insulating the transducer, or eliminated by choosing a transducer that is compensated over a wide temperature range. Using individual pressure transducers located at desired sampling elevation also worked very well. This technique can be used at any time, but is necessary under circumstances where very rapid measurements are desired for locations at depths. Because downhole temperatures are very stable, temperature sensitivity is not a major concern with this method. However, the sensors must be calibrated before emplacement if comparison of relative pressures at different sampling locations is desired. An offset drift observed in the gauges tested would render them unusable for long term monitoring, but higher precision transducers are available.

As expected, the downhole temperatures measured were very stable even at shallow depths. The platinum resistance thermometers tested proved to be more stable and precise than thermocouples measuring temperatures to  $\pm .01^{\circ}\text{C}$ . The ability to precisely measure borehole temperature is necessary, for example, in performing near-surface soil moisture flux measurements.

The three sensors tested to measure the hydrologic matric potential included a relative humidity sensor, a thermocouple psychrometer, and a soil moisture (gypsum) block. The three types were chosen to assure that the operating range of one or more of the sensors would be adequate to measure the expected matric potential of -5 to -30 bars at the CWL. The soil's moisture content proved to be higher than expected, resulting in a measured hydrologic potential of -0.2 to -0.3 bars at the 6-foot sampling elevation, and -0.9 to -1.0 bars at the 51-foot elevation. These potentials were out of range of the relative humidity sensors, but were measurable by both the thermocouple psychrometers and gypsum blocks. The time required to reach equilibrium was up to 72 hours or longer for all of the sensors. The equilibration time of

the gypsum blocks was found to be highly dependent on the state of the block, saturated versus unsaturated, when deployed.

The four chemical sensors integrated and tested with the SEAMIST™ system included Adsistors™, Gore-Sorbers, Dräger tubes, and litmus or pH paper. Each of the sensors detects or measures the chemical contaminants in a sufficiently different way so that direct comparison of the results difficult.

Adsistors™ detect hydrocarbon contaminants by sensing a resistance change caused by the contaminants adsorbing onto the sensor. The Adsistor™ is a gross contaminant monitoring technique adsorbing all hydrocarbons. However, the resistance change sensed by the Adsistor™ varies with each hydrocarbon, which can cause the results recorded with the sensor to be skewed toward an individual contaminant. Further testing of the sensors' response to individual contaminants is needed before results from the Adsistors™ can be fully evaluated. Additional work must also be done to optimize the technology before it can be used in quantitative monitoring applications. The sensor's housing must be designed so that baseline resistances are not affected by sensor position, and temperature sensitivity of the sensors must be evaluated. The manufacturer of Adsistors™ is presently addressing these concerns. However, for monitoring relative changes in contaminant concentrations over time, the sensors available now are adequate. Positive features of this sensor are that it is sensitive to less than 100 ppm hydrocarbon concentration variations, is reversible at these low concentrations, operate at depth, and is presently available for use. Adsistors™ are seen as a potentially simple and inexpensive method of contaminant monitoring.

Gore-Sorbers are passive absorbent charcoal modules. Analysis of a module shows the integrated amount of contaminants absorbed over the time the module is exposed to the contaminants. Because the sensors integrate the contaminant by which concentration over time, they are especially useful in detecting very small concentrations. Gore-Sorbers were emplaced for 12 days at nine sampling elevations in the CWL. Results showed that the contaminant concentrations in general increased with depth, although at the more shallow sampling elevations higher concentrations of 1,2 DCB and acetone were measured.

Dräger tubes are colorimetric indicating tubes used to sample for the presence of a specific contaminant. They are used with SEAMIST™ via gas sampling tubes that run between the surface and the desired sampling elevation. Because they sample for specific contaminants and use gas sampling ports to access the in-situ soil vapor, they are very similar to gas chromatograph analysis. Using the Dräger tubes to sample for toluene resulted in a non-detect at each elevation. Sampling for TCE showed peak concentrations at the 31- and 51-foot elevations. Results correspond well with GC analysis. While a GC analysis is arguably more accurate than Dräger tubes, the low cost and simplicity of the Dräger tubes makes them ideal for periodic monitoring. For volatile contaminants the effectiveness of remediation activities can be monitored and indicate when to conduct more accurate GC analysis.

Litmus paper was used in an effort to determine the locations of chromic acid contamination in the UCAP3 borehole. The paper was quickly and easily emplaced and began indicating after only a very short emplacement time (10 minutes). However, the concentration of the acid was too low to be detected.

The SEAMIST™ systems were readily integrated with portable and automatic gas analysis equipment. The SNL automated GC accurately measured concentration histories at multiple elevations of the membranes. The SNL ultraviolet fluorometer showed potential as a conceptually simple but very sensitive analysis device.

The focus of this project was the demonstration of the SEAMIST™ system's deployment versatility. All these sensors and samplers were readily integrated with the SEAMIST™ system. Standard available sensors were used in a variety of shapes and sizes. Comparison of laboratory and field test results indicate that the membrane deployment did not appear to degrade the performance of the sensors and samplers.

By combining previous measurements of gas permeability in the UCAP boreholes with pressure gradients recorded from the SEAMIST™ membrane/sensor system in these boreholes, significant vapor movement was predicted over the one week recording period. Several hundred centimeter displacements are estimated in the high permeability regions and tens of centimeters in other regions indicating that displacement scales with permeability. The recording period occurred during a low pressure cycle, which resulted in an initial upward vapor movement, in most cases, upward followed by downward movement. The uncertainties in this estimating technique result from the uncertainty of the permeability measurements and the accuracy of the pressure gradient data.

The data were also used to substantiate and support the SEAMIST™ system capabilities. The recorded pressures on the SEAMIST™ systems were compared to the available measured pressure from Geoprobe points at similar depths in the area. The SEAMIST™ measurements were virtually indistinguishable from the Geoprobe data, indicating that for this application the SEAMIST™ borehole seal quality was at least as good as the seal afforded by a grouted Geoprobe installation. The recorded data was used to estimate the vertical permeability of the soil using a time series technique. These analyses resulted in a gross vertical gas permeability of about 10 darcies, a very credible average of the measured in-situ permeabilities used in the calculations.

The advective component of the vapor movement is one factor in the transport of volatile contaminants in soil, and by itself will not necessarily result in a net vapor movement over time because of its cyclic nature. The next step to understand plume movement is to use these types of measurements with tracer injections and automated gas analysis at multiple points to evaluate movement of contaminant species in the soil. Laboratory tests and analysis have shown that when lateral diffusion is coupled with the cyclic vertical motion in heterogeneous media, an irreversible displacement of contaminants in the soil vapor can occur. Tracer studies could be used to detect and verify this phenomena.

From an experimental standpoint, some changes in the instrumentation are required. The selection of a less temperature-sensitive barometric pressure transducer and use of narrow range differential pressure transducer to record the difference between surface and in-situ gas pressure would allow a factor of ten increase in the general measurement accuracy and pressure gradient measurement precision.

SEAMIST™ systems were also provided to support slant and directionally drilled boreholes formed beneath two other contaminated sites. A 160-foot-long, 4-inch-diameter multiport vapor sampling system was fabricated and installed beneath the CWL "60's pits". The longest membrane to date (400 feet) was installed inside 4-inch perforated casing emplaced in a directionally drilled hole beneath the Kirtland Air Force Base RB-11 landfill. Both these systems supported soil gas VOC measurements.

## REFERENCES

Daniel B. Stephens & Associates, Inc. 1989. Laboratory Analysis of Soil Hydraulic Properties from Chemical Waste Landfill Cap Verification Project. Albuquerque, NM. Daniel B. Stephens & Associates, Inc.

IT Corporation. 1992. Unlined Chromic Acid Pit (UCAP) Site Investigation.

Peterson, E.W., K. Lie, and R.H. Nilson. 1987. "Dispersion of Contaminant During Oscillatory Gas-Motion Driven by Atmospheric Pressure Variations." Fourth Symposium of Containment of Underground Nuclear Explosion. United States Air Force Academy, Colorado Springs, Colorado; September 21-24, 1987. Proceedings Volume 2. CONF-870961.

Phelan, J.M. 1993. Field Measurements of Soil Air Permeability at the Chemical Waste Landfill. Albuquerque, NM: Sandia National Laboratories, Environmental Restoration Technologies, Department 6621.

Nilson, R.H., E.W. Peterson, and K.H. Lie. 1991. "Atmospheric Pumping: A Mechanism Causing Vertical Transport of Contaminated Gases Through Fractured Permeable Media." Journal of Geophysical Research. Vol. 96, no. B13, pp. 21,933-21,948.

**Intentionally Left Blank**

**Intentionally Left Blank**

## APPENDIX A. PROCEDURES

### **Gore-Sorber™ Procedure**

1. Fully extend SEAMIST™ membrane in the laboratory.
2. Begin retrieving membrane until first Gore-Sorber™ holder is about to be inverted.
3. Remove sorber from vial and place inside holder.
4. Immediately reseal vial and store in a safe place.
5. Repeat steps 2 through 4 until all Gore-Sorbers™ are on the membrane.
6. Continue inverting the membrane until it is fully contained in the SEAMIST™ canister.
7. Seal the end of the canister.

### **Gas Sampling Procedure**

The procedure used to collect the samples consisted of four steps involving a Xitech gas sampling unit. These steps were:

- 1) **Purge the line** - approximately 1-liter of gas was withdrawn into a Tedlar bag from the Teflon tubing line connected to a gas withdrawal port on the SEAMIST™ membrane (this is approximately 16 times the purge volume of the longest sample line).
- 2) **Collect 1-liter sample** - using the same method to purge the line, an approximate 1-liter sample is withdrawn into a Tedlar bag.
- 3) **Sample gas using Dräger tube** gases from the 1-liter Tedlar bag are withdrawn through a Dräger tube using the manufactures instructions for volume of gas flow specific to the tube type.
- 4) **Record data** - The length of the reactant in the tube which undergoes a color change is compared to the calibrated markings on the tube corresponding to gas concentration level and the results are recorded.

**Intentionally Left Blank**

## Distribution

### Federal Agencies

|   |                                  | <b>Internal</b> |                     |
|---|----------------------------------|-----------------|---------------------|
|   |                                  | <u>MS</u>       | <u>Org</u>          |
| 2 | US Department of Energy          | 1               | 6621 Library        |
|   | Office of Technology Development | 6               | C.V. Williams       |
|   | Attn: S. Chamberlain, EM-551     | 1               | G. Allen            |
|   | Cloverleaf Center                | 5               | Technical Library   |
|   | 19901 Germantown Rd              | 1               | Print Media         |
|   | Germantown, MD 20874-1290        | 2               | Document Processing |
| 1 | US Department of Energy          | 1               | for DOE/OSTI        |
|   | Albuquerque Operations Office    | 9018            | Central Technical   |
|   | ETN                              |                 | Files               |
|   | Attn: Dennis Olona               |                 |                     |
|   | Pennsylvania/H Street            |                 |                     |
|   | Albuquerque, NM 87116            |                 |                     |

### Corporations

9 Science & Engineering Assoc., Inc.  
Attn: William Lowry  
1547 Pacheco, Suite D1  
Santa Fe, NM 87501

### Libraries

1 Thomas Branigan Library  
Attn: D. Dresp  
106 W. Hadley St.  
Las Cruces, NM 88003

1 Government Publications  
Zimmerman Library  
University of New Mexico  
Albuquerque, NM 87131